VOL. 86/JUN. 1999

MITSUBISHI ELECTRIC ADVANCE

Satellite Edition

Courtesy of NASDA

MITSUBISHI ELECTRIC

A Quarterly Survey of New Products, Systems, and Technology

●Vol. 86/Jun. 1999 Mitsubishi Electric **ADVANCE**

Satellite Edition

CONTENTS

TECHNICAL REPORTS

OVERVIEW

Mitsubishi Electric's Place in Space **1**
by Hiroshi Kimura

Data Relay Test Satellites **2**
by Hiroyuki Ichino, Naoto Shikagawa and Keisuke Ozawa

USERS, An Unmanned Space Experiment Recovery System **5**
by Masao Sato and Tetsuo Yamaguchi

Space Radio Monitoring System **8**
by Yoshimasa Oh-hashi and Morio Higa

N-STAR Ka-Band Antenna **11**
by Takao Itanami, Kenji Ueno, Izuru Naito and Yuji Kobayashi

Adaptive Attitude Control of Spacecraft with Movable Antennas **14**
by Katsuhiko Yamada and Shoji Yoshikawa

Digital Circuit Multiplication Equipment Based on Intelsat Specifications **17**
by Nobuhiro Gencho and Mitsuhiro Takemoto

A Digital Satellite Newsgathering System **20**
by Masamizu Hinata and Tatsuhiro Oba

TECHNICAL HIGHLIGHTS

Automatic Rendezvous and Docking Experiments **23**
by Hiroshi Koyama and Makoto Kunugi

A Very Small Aperture Terminal **25**
by Shuji Nishimura and Seiya Inoue

A Notebook-Size Satellite Terminal **27**
by Katsumi Tsukamoto and Atsushi Manzaki

MITSUBISHI ELECTRIC OVERSEAS NETWORK

"Advance" to Become Online Magazine

Readers are advised that the September, 1999, edition of Advance will be the last one to be printed as a traditional magazine. From December, Advance will continue to be available, as it is now, at the Mitsubishi Electric global homepage website (URL http://www.mitsubishielectric.com/ghp_japan/corporate_profile/advance/advance_index.html). It is hoped that the move to online format will speed publication and enable readers to print out only those articles of special interest to them.

Our cover shows Engineering Test Satellite-VII (the pair facing each other, below) and a Data Relay Test Satellite (above). ETS-VII is intended to acquire the basic technologies of rendezvous docking and space robotics which are essential to future space activities such as retrieval, resupply and exchange of equipment on orbit. In July and August 1998, it succeeded in the world's first unmanned rendezvous docking.

Two DRTS satellites, which are to be launched in 2000 and 2002, will make it possible for a ground station to communicate with spacecraft (satellites and rockets) without the help of other ground stations in most of their flight area.

Editorial Inquiries

Masakazu Okuyama
Corporate Total Productivity Management
& Environmental Programs
Mitsubishi Electric Corporation
2-2-3 Marunouchi
Chiyoda-ku, Tokyo 100-8310, Japan
Fax 03-3218-2465

Product Inquiries

Yasuhiko Kase
Global Strategic Planning Dept.
Corporate Marketing Group
Mitsubishi Electric Corporation
2-2-3 Marunouchi
Chiyoda-ku, Tokyo 100-8310, Japan
Fax 03-3218-3455

Orders:
Four issues: ¥6,000
(postage and tax not included)
Ohm-sha Co., Ltd.
1 Kanda Nishiki-cho 3-chome
Chiyoda-ku, Tokyo 101-0054, Japan

Mitsubishi Electric Advance is published quarterly (in March, June, September, and December) by Mitsubishi Electric Corporation.

Overview

Mitsubishi Electric's Place in Space

*by Hiroshi Kimura**

In recent years, American and European aerospace companies have been undergoing a worldwide realignment that is concentrating them into a few, large enterprise groups. This process suggests that only those enterprises with well-balanced technical, financial and sales strengths will survive to participate in the development of the space industry in the 21st century.

In the Space Systems Division of Mitsubishi Electric, our strategy is based on possession of powerful key technologies for satellite communication, earth observation and aerospatial infrastructure, and taking full advantage of our position as an integrated electrical and electronic manufacturer. The strategy aims to achieve total vertical integration, enabling the company to offer our customers one-stop shopping from the space segment itself through ground control to the end user. Our efforts are specifically directed at supporting customers with the best, fastest and lowest cost services, and at configuring systems with the flexibility to ensure complete satisfaction.

In 1998, the two ETS-VII satellites *(Orihime* and *Hikoboshi)* successfully achieved the world's first unmanned docking rendezvous, thus flight testing a key technology for the unmanned H-II transfer vehicles (HTVs) that will supply the future International Space Station. A key technology for the next generation of communication satellites—the data relay test satellite (DRTS)—has completed the protoflight model stage and they have now entered their final acceptance tests.

The unmanned space experiment recovery system (USERS) has already completed customer design review, and represents significant progress towards the implementation of a low-cost recoverable system. Integration has already begun in preparation for the launch of the ADEOS-II satellite in 2000. Orders for commercial satellites include one from OPTUS, the Australian cable and wireless company, for the OPTUS-C1, a new type of communication satellite.

We are committed to working with our customers to conceive, propose and provide the satellite systems for the 21st century.

**Hiroshi Kimura is General Manager of the Space Systems Division.*

Data Relay Test Satellites

*by Hiroyuki Ichino, Naoto Shikagawa and Keisuke Ozawa**

NASDA plans to launch two data relay test satellites, DRTS-W in the year 2000 and DRTS-E in 2002. The two medium-sized geostationary satellites feature enhanced interorbit communications support and control capabilities, and will form part of an experimental system to setup and test future communication satellites.

The DRTS satellite system includes interorbit communication equipment (ICE) payload, a satellite engineering bus consisting of eight subsystems, technical data acquisition equipment, and monitoring camera equipment. All of the equipment is designed from the ground up to provide a measure of redundancy. Table 1 lists the major parameters and Fig. 1 shows the flight configuration of the satellite.

The DRTS has a number of design features that will increase the proportion of the satellite's total weight that can be devoted to its communications equipment payload. In addition, the satellite has acquisition and tracking capabilities enhanced to support the high-accuracy requirements of future interorbital communication systems. The capacity of the return channel in the Ka band interorbit communication equipment has been boosted. The antenna aperture efficiency has

Table 1 Major Specifications of DRTS

Physical dimensions	
Satellite body	2.39 × 2.16 × 2.22m (x, y, z)
Interorbital link antenna	3.6m aperture diameter
Feeder link antenna	1.80m aperture diameter
Satellite with antennas and paddles deployed	6.61 × 16.36 × 6.19m (x, y, z)
Satellite mass	
Prelaunch	About 2,700kg
Dry weight	About 1,270kg
Payload (ICE)	About 310kg
Power generation capacity	Better than 2,115W over mission life
Mission life	7 years
Attitude control	Controlled-bias momentum system
Geostationary position	
DRTS-W	90°E (tentative)
DRTS-E	170°W (tentative)

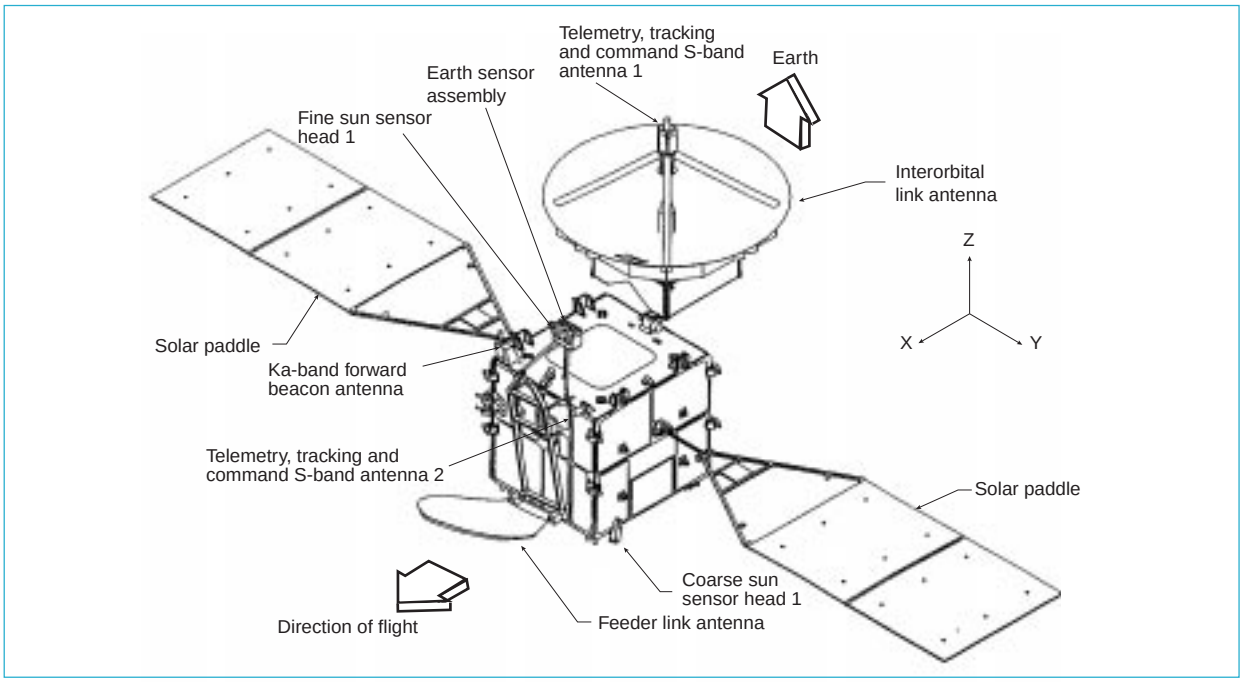

Fig. 1 DRTS configuration in orbit.

**Hiroyuki Ichino and Naoto Shikagawa are with the Kamakura Works and Keisuke Ozawa with NASDA.*

Table 2 Bus Subsystem Specifications

Telemetry, tracking and command S-band USB and Ka bands, data buses with central and remote-interface units
Electric power supply 32~51.5V floating bus, two 50Ah NiH_2 batteries, digital sequential shunt, better than 2,075W over mission life from solar paddles in sunlight, better than 1,866W in shadow, better than 3,710W from batteries in polar orbit
Solar paddle system Rigid ultralightweight panels, 2,115W power generation capacity over mission life, high-performance 100µm Si NRS/BSF photovoltaic cells
Attitude control system Controlled-bias momentum system using adaptive algorithm with integrated antenna control. Sensors include integrating gyroscope, earth sensor and coarse and fine sun sensors. Actuators include momentum and balance wheels, and thrusters. Roll and pitch are within ±0.05° and yaw within ±0.15° in normal operating mode, varying within ±0.07° and ±0.20°, respectively during antenna movements or transient attitude control maneuvers. Roll and pitch are within 2° during apogee engine firing.
Structural system Central cylinder system using CFRP monocoque shell and struts weighing 185kg.
Thermal control system Combined system using passive insulating laminate and an active system of heaters and heat pipes in the RF compartment and along the satellite's north and south surfaces.
Unified propulsion subsystem Two-fluid 500N apogee-kick engine combined with 1 and 20N one-fluid gas jet thrusters, adjustable pressure blowdown, up to 973kg of N_2H_4 propellant, up to 640.8kg of mixed oxides of nitrogen 3%-NO (MON-3), 200mN DC ion engine for stationkeeping.
Integrated hardware subsystem Components include power distribution unit, power-divider ordnance controller, light-load mode units and heater control electronics. Also included are wire harnesses, RF cables, waveguides, separation switches, brackets, fasteners, and pyrotechnical products.

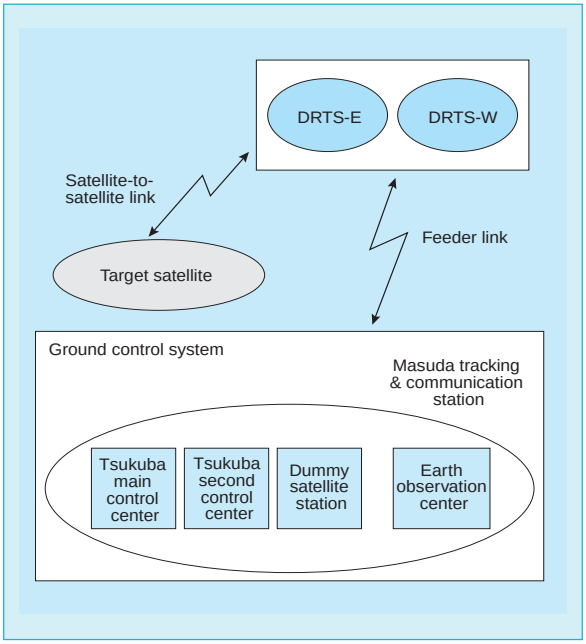

Fig.2 DRTS experimental space network system.

been increased to conduct experiments with more channels and high data-rate transmission. The tracking receiver features increased bandwidth and reduced noise.

The satellite bus design will incorporate technologies from COMETS and other test satellites to lower development costs wherever possible. Table 2 lists some of the main performance specifications of the satellite bus system.

Interorbit Communication Equipment

The ICE subsystem is the satellite's primary payload. It consists of a Ka- and S-band interorbit antenna, five transponders and a Ka-band feederlink antenna.

NASDA will use the satellite to conduct experiments with a number of domestic satellites: the Advanced Earth Observing Satellite II (ADEOS-II), the Advanced Land Observing Satellite (ALOS), the Japanese Experimental Module (JEM), the Optical Interorbit Communications Engineering Test Satellite (OICETS), the H-II Transfer Vehicle (HTV), H-II Orbiting Plane X (HOPE-X) and H-IIA. NASDA is also planning experiments with NASA and ESA.

Satellite Experiments Interface

Satellite developers will be able to conduct experiments with their satellites' ICE subsystem from the DRTS earth station that will be developed as part of the project. Fig. 2 shows the feeder and interorbit communication links that comprise the network and its interfaces. Table 3 describes the interorbital link. The DRTS earth station will make some of its data interfaces available to satellite developers for systems compatibility testing. Table 4 lists these interface functions.

ICE Functions and Performance

The ICE subsystem supports the following functions for data communications and acquisition and tracking: S-band single access (SSA) forward and return links, Ka-band single access (KSA) forward and return links, and Ka-band forward beacon links. Forward tests consist of transmitting data from the ground station to the DRTS and on to the target satellite. Return tests involve transmitting data from the target satellite to the DRTS and on to the ground station. SSA and KSA are coherent systems that link phase synchronous pilot signals from the ground station.

The DRTS can communicate with satellites located within ten degrees of the earth's center, which corresponds to altitudes up to 1,000km.

The system provides S- and Ka-band test sat-

Table 3 Communication Link Parameters for User Spacecraft

Item	SSA link	KSA link
Frequency		
Forward	2,025~2,110MHz (100kHz steps)	23.175~23.545GHz (1MHz steps)
Return	2,200~2,290MHz (100kHz steps)	25.450~27.500GHz (100kHz steps)
Forward beacon	—	23.175~23.545GHz (1MHz steps)
Polarization	Right or left (same for transmitter and receiver)	Right or left (independent for transmitter and receiver)
Transmit EIRP (1dB steps)		
Forward	38.0~46.0dBw	48.0~62.0dBw
Forward beacon	—	30.5dBw (wide beam), 38.4dBw (narrow)~48.0dBw
G/T	8dB/K	27dB/K
Relay bandwidth		
Forward	20~24MHz	50~60MHz
Return	13.5~16.5MHz	300~360MHz
Forward beacon	—	10~12MHz

ellite program tracking functions. The on-board tracking receiver uses the KSA return data signal to control the interorbital link antenna for acquiring and tracking the test satellite. There is also a scan and search program. The satellite will forward a Ka-band beacon signal from the ground to test a target satellite's acquisition and tracking capabilities. The interorbital link antenna can also be controlled by manual ground commands to point at angles up to 15 degrees from the earth's center.

The satellite provides functions for tuning the frequencies of the SSA and KSA links, both forward and return. The satellite can also store ten sets of acquisition and tracking program parameters on board, allowing it to conduct tests of multiple satellites.

The DRTS' ICE subsystem has an enhanced version of the technologies developed for that of the COMETS satellites, and is designed to allow experiments with many kinds of satellites.

The interorbital link antenna gain and sidelobe performance have been boosted by modifying the antenna configuration and stay design. Errors related to thermal expansion of the antenna have been reduced.

The Ka-band transponders support a wider bandwidth and higher transmission power to increase data capacity. The receiver features increased dynamic range, while phase noise in the frequency synthesizer has been reduced. Feeder antennas for both DRTS-W and DRTS-E are designed to allow changes to the orbital position. Pointing control is handled by the attitude control system.

The slew and pull-in time for satellite acquisition have been shortened. Tracking can be performed by manual pointing commands to support communications with satellites in variable orbits under 1,000km.

Table 4 Space Network Service Capabilities

Item	SSA link	KSA link
Modulation		
Forward	UQPSK	UQPSK, QPSK, BPSK
Return	SQPN, SQPSK, QPSK, BPSK, UQPSK	SQPN, SQPSK, QPSK, BPSK, UQPSK
Encoding and demodulation		
Forward	Typically none used	Typically none used, and convolutional encoding, Viterbi decoding (R = 1/2, K = 7) with plans for JEM support
Return	Convolutional encoding, Viterbi decoding (R = 1/2, K = 7)	Convolutional encoding, Viterbi decoding (R=1/2, K=7) with plans for JEM support. Reed-Solomon decoding (255, 223) with plans for ALOS support. Reed-Solomon decoding (255, 223) or none used with ADEOS-II support.
Data transfer rate		
Forward	100bps~300kbps	100kbps~50Mbps
Return	100bps~6Mbps	100kbps~240Mbps
Transmission quality (BER)		
Forward	1×10^{-6} or better	1×10^{-6} or better under 300kbps, 1×10^{-5} or better over 300kbps
Return	1×10^{-5} or better	1×10^{-6} or better

Detailed design of the DRTS systems has been completed, and production of protoflight model DRTS-W is underway toward a launch in 2000. ❑

USERS, An Unmanned Space Experiment Recovery System

*by Masao Sato and Tetsuo Yamaguchi**

USERS is a reusable spacecraft being developed by Japan's Ministry of International Trade and Industry, the Organization for Development of New Energy and Industrial Technologies, and the Institute for Unmanned Space Experiment Free Flyer (USEF). USERS is intended to support applications of the space environment. The spacecraft will consist of two major components, a reentry module (REM) and a service module (SEM). The REM will contain an electric furnace for experimental production of superconducting materials and will return to earth after the conclusion these experiments. The SEM will provide electricity and other resources to the REM and will house its own experimental equipment. The SEM will be used to develop a multipurpose compact satellite bus capable of applications in high, medium and low orbits.

The satellite bus will have the following design features to support a wide range of applications and low production costs. The satellite size and weight will be reduced by use of a software-intensive integrated control system that will lower reliance on special-purpose hardware. Mass-produced components will qualified in mission equipment and eventually incorporated into the satellite bus. Finally, project management will be simplified by adopting CALS technologies, reducing paper documentation, introducing 3D CAD systems, and automating test procedures.

USERS will be launched together with another satellite by a Japanese-developed H-IIA rocket from NASDA's Tanegashima Space Center in winter, 2000 and carried to an orbital altitude of about 500km. The REM will carry out its six-month mission then separate from SEM and return to earth while the SEM will continue an independent two-and-a-half year mission (Fig. 1). Mitsubishi Electric has been awarded the primary development contract for the spacecraft system and is a supporting contractor for the overall USERS system.

The USERS Missions

USERS has two missions. The REM will carry units for low-power experimental manufacture of superconducting materials in the space environment and return these units and the materials they contain to earth at the conclusion of the mission. Afterwards, the SEM will remain in orbit to conduct in-flight qualification testing of space equipment. SEM's mission equip-

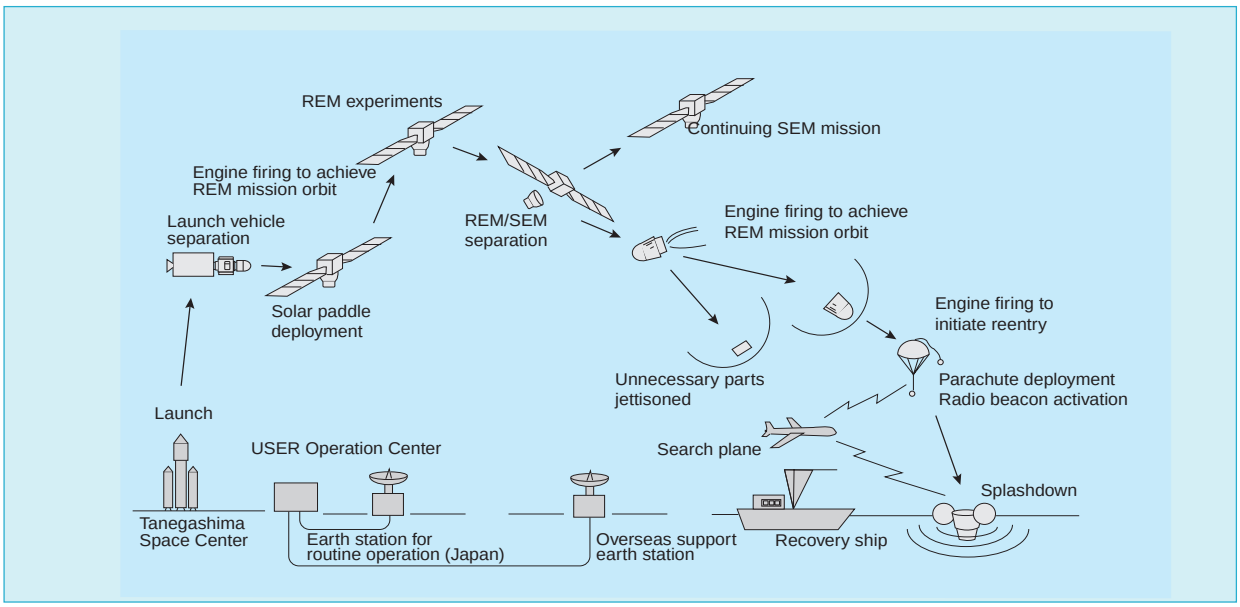

Fig. 1 USERS flight plan.

**Masao Sato and Tetsuo Yamaguchi are with the Kamakura Works.*

ment is being designed to be developed cheaper, faster and better than typical custom-developed hardware. Five equipment designs will be selected from those proposed by the manufacturers participating in the USERS program. Mitsubishi Electric has proposed an advanced star sensor system, which it is preparing to develop and test alongside the satellite bus systems.

The USERS Spacecraft

Table 1 lists basic specifications of the USERS spacecraft and Fig. 2 illustrates the craft. The 800kg SEM will be supporting its 100kg internal payload as well as the 700kg REM (which carries 150kg of mission equipment.) SEM is

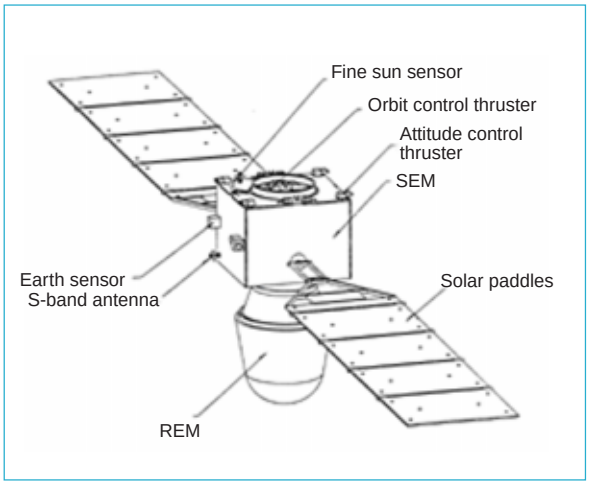

Fig. 2 An illustration of the USERS spacecraft.

Table 1 Major Specifications of the USERS Spacecraft and Mission

Launch	By H-IIA rocket from Tanegashima Space Center in winter, 2000
REM recovery	Ocean recovery near Ogasawara Islands six months after launch
Launch weight	1,500kg (SEM: 800kg, REM: 700kg, assuming 500km orbit)
Orbit	Circular orbit, 500km altitude, 30.4° elevation
Mission life	6 months for coupled REM/SEM mission, 2.5 years for independent SEM mission
Microgravity environment	Less than 10^{-5}G in sun-facing mode
SEM	
Payload	Five types of equipment designed for high-performance fast and inexpensive development (100kg max, 200W)
Structural thermal control system	Central cylinder and panels with active thermal transport Integrated spacecraft control system
Data processing	CCSDS compliant packet command/packet telemetry
Data recorder	1GB semiconductor memory
Attitude control	Sun-facing mode (±1°), earth-facing mode, inertial guidance (for REM separation maneuver)
System management	Power and heater control
Attitude and orbit control equipment	Inertial reference unit, sun sensor, earth sensor, reaction wheel, magnetic torquer, GPS receiver
Communication system	
Commands	4kbps USB system
Telemetry	USB or high-speed S-band system (switchable), 256kbps max
Power system	50Ah nickel hydride battery, 2,450W solar paddles
Thrusters	1N and 23N single-fluid hydrazine engines, 126kg propellant
Environment measurement instruments	Radiation counter and dosimeter
REM	
Payload	Superconducting materials experiment, reentry environment measurement (150kg, 600W total)
Attitude control	Dual-spin stabilizer with 50Nms momentum wheel and inertial reference
Power system	NiCd battery (charged prior to separation from SEM)
Communication system	S-band telemetry and command system
Thermal protection	Ablation system
Recovery system	Parachute, GPS beacon, ARGOS transmitter
Solid-fuel rockets	Orbit separation (RBM, 1), spin (3), despin (3), tumble (1)
Environment measurement instruments	Microgravity meter

therefore supporting a total of 800kg of mission equipment, more than half of the spacecraft's weight. SEM and REM will be mechanically and electrically coupled at launch. Although USERS is intended for a circular orbit at an altitude of about 500km and an elevation of 30° , the choice of orbits will be affected by the requirements of its launch partner satellite. USERS will therefore carry a single-liquid hydrazine thruster that will enable it to boost itself into its mission orbit.

Soon after REM separates from SEM, its orbital separation motor will ignite to initiate reentry. SEM will subsequently continue its in-flight qualification mission. REM's mission life is six months; the SEM mission will last a total of three years.

SEM will be supplying high-quality electric power and other resources for REM's superconducting material tests. In addition to supporting REM and assisting its reentry, SEM will be used to develop a standard bus for light (500~1,000kg) satellites to be used through the early years of the new century. SEM's control system will need to be able to reconfigure itself to adapt to the radically different orbital control dynamics, power management and thermal control characteristics before and after REM separation.

The key to reducing the recurring costs for the compact standard satellite bus is the introduction of an integrated spacecraft controller (ISC). The ISC combines the previously separate functions of data processing and attitude control, and integrates power and thermal management functions as well. Hardware size and weight is reduced by implementing functions in software and reducing the usual multiplicity of interfaces to a bare minimum. This integration will allow use of the same basic hardware design in subsequent missions. Mission-specific changes will be made primarily at the software level. Implementing functions at the software level has the added benefit of facilitating development of automatic test procedures.

The superconducting material experiment will simultaneously require a high-current supply for the furnace and a highly regulated low-power supply for control. To generate maximum power, the spacecraft will adopt a sun-facing attitude that will maintain the solar paddles at 90° to incident solar radiation. The paddles will be fixed relative to the spacecraft to avoid the attitude disturbances associated with paddle drive operations. Attitude control will be implemented by a reaction wheel and magnetic torquer to maintain a stable microgravity environment on the order of 10^{-5}G.

The SEM can also be operated in an earth-facing attitude control mode to support earth-observation, measurement and communication missions. USERS is also designed to operate in earth-facing mode during orbital control maneuvers and during and following REM separation. In earth-facing mode, the solar paddle drive mechanism operates to orient the solar paddles toward the sun, ensuring a supply of electrical power. Modifications to the thermal control software to maintain appropriate heat balance are all that is needed to adapt to these various orientations.

In addition to developing the new technologies needed to manage spacecraft separation and capsule recovery operations, USERS is providing a vital test bed to lower the recurring costs of spacecraft development. ❑

Space Radio Monitoring System

*by Yoshimasa Oh-hashi and Morio Higa**

The worldwide growth in satellite-based telecommunications and broadcasting is increasing the likelihood of radio interference in satellite-to-earth and satellite-to-satellite communications. This report describes a proposed space radio monitoring system that will measure satellite orbits while monitoring satellite radio emissions.

Satellites are increasingly used to provide sophisticated radio communication capabilities for business and subscriber services. As satellites' orbits and communication frequencies get closer, the risk for interference increases. Japan's Ministry of Posts and Telecommunications (MPT) is developing satellite orbit and radio emissions monitoring facilities that will help prevent interference and support effective use of satellite orbits and communication frequencies. The MPT is commissioning a fixed monitoring station that will monitor the L, S, C, Ku and Ka bands used by geostationary satellites.

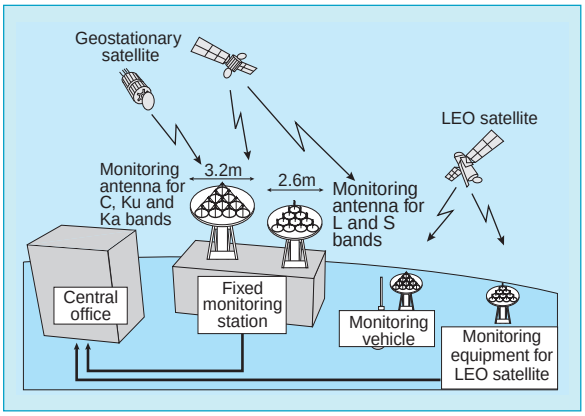

Fig. 1 Configuration of space radio monitoring system.

System Configuration

Fig. 1 illustrates the proposed system while Fig. 2 shows a block diagram of the fixed monitoring station. Two antennas arrays each consisting of ten elements will measure satellite orbits and monitor radio emissions. One array will monitor the L and S bands, the other the C, Ku and Ka

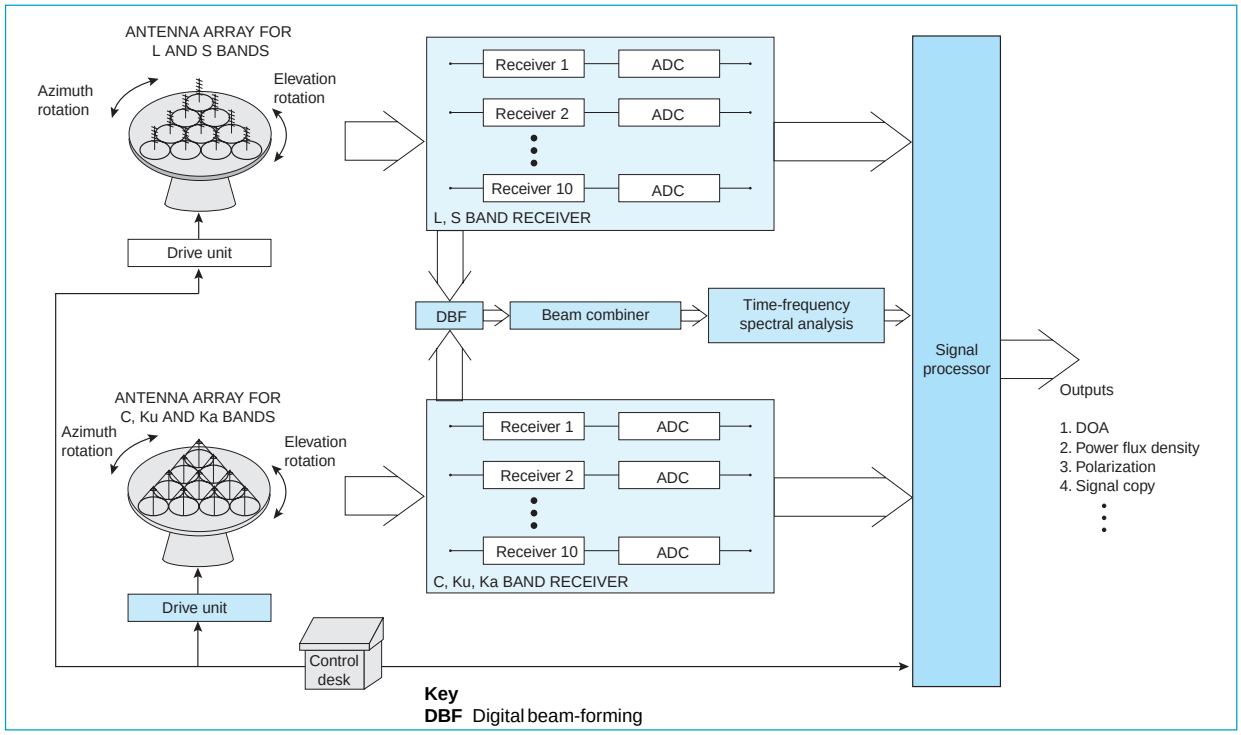

Fig. 2 Block diagram of a fixed monitoring station.

**Yoshimasa Oh-hashi and Morio Higa are with the Kamakura Works.*

bands. Fig. 3 shows the configuration of the antenna array. The signals from each of the elements are individually amplified, frequency converted and passed through an ADC in preparation for the signal processor. The signal processor will employ an extended version of the ESPRIT algorithm (estimation of signal parameters via rotational invariance techniques)[1] to determine direction of arrival (DOA), power flux density and polarization of incident satellite radio signals, and to copy signals.

Features

HIGH RESOLUTION DIRECTION DETERMINATION. The extended ESPRIT algorithm enables the monitoring station to precisely and instantaneously determine satellite azimuth and elevation from received radio signals, despite the antennas' relatively small aperture.

DISTINGUISHING BETWEEN MULTIPLE SATELLITES. When two or more satellites are in the antenna's field of view, the extended ESPRIT algorithm easily distinguishes and locates the satellites, which is not possible using the monopulse or step-track methods. Resolution is higher than the multiple signal classification (MUSIC) algorithm[2] while the computing cost is much lower.

WIDE FIELD OF VIEW. By using the extended ESPRIT algorithm with multiple small-aperture antenna elements, the system achieves a wider field of view than is possible using previous technology with a large-aperture antenna.

COPYING MULTIPLE SIGNALS. An eigenspace projection algorithm[3] makes it possible to extract individual signals when multiple radio sources are within the antenna's field of view.

SUPPRESSION OF FALSE DOAS. The antenna elements' aperture must be larger than the satellite transmission wavelength in order to receive weak signals, however the present of grating lobes can lead to computation of spurious DOAs. An original angle diversity reception system suppresses these false DOAs.

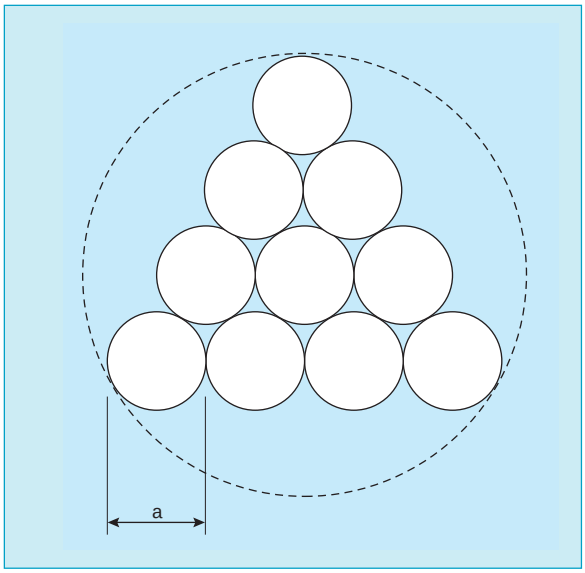

Fig. 3 Triangular array of ten antenna elements.

Technology Elements

Figs. 4 and 5 show numerical simulation results for DOA estimations of the extended ESPRIT algorithm for signals in the L and Ku bands. Fig. 4 assumes the following conditions:

Frequency	L band (1.525GHz)
Antenna element diam.	0.65m
Antenna element C/N	–15 ~ 0dB
First signal source	0° azimuth, 0° elevation
Second signal source	7° azimuth, 0° elevation
Array manifold error for each element within a 3dB beamwidth	
Amplitude error	1.6% (0.07dB)
Phase error	1.3°

In Fig. 5, the conditions are:

Frequency	Ku band (17.7GHz)
Antenna element diam.	0.8m
First signal source	0° azimuth, 0° elevation
Second signal source	0.4° azimuth, 0° elevation
Array manifold error	as above

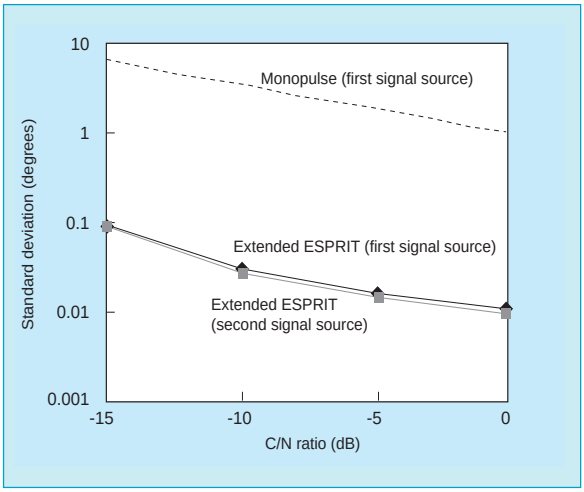

Fig. 4 Comparison of extended ESPRIT and monopulse DOA estimation for f = 1.525GHz.

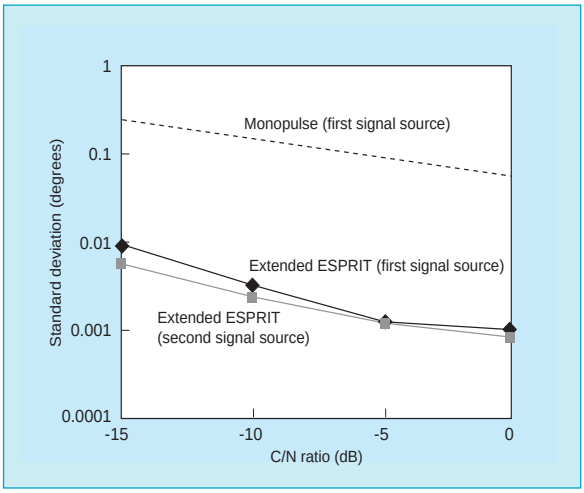

Fig. 5 Comparison of extended ESPRIT and monopulse DOA estimation for f = 17.7GHz.

The broken lines in Figs. 4 and 5 show the DOA estimation using the monopulse method with the first signal source. The model assumes the antenna aperture shown by the broken line in Fig. 3. The extended ESPRIT algorithm can perform multiple simultaneous DOA estimation, resolving signal sources with accuracy superior to the monopulse method.

The proposed monitoring station will combine the versatility of array antennas with a superior signal-processing algorithm to identify the DOA of signals from satellites. The MPT is considering the use of these capabilities to minimize the risk of radio interference disrupting satellite communications. ❑

References

[1] Y. Oh-hashi, "High-Performance Space Monitoring System with Small Antennas Using Superresolution Algorithms," in Proc. International Space Radio Monitoring Workshop sponsored by Japan's Ministry of Posts and Telecommunications, Tokyo, Japan, Nov. 1998.

[2] R.O. Schmidt, "Multiple Emitter Location and Signal Parameter Estimation," IEEE Trans. on AP, vol. AP-34, no.3, March 1986.

[3] Y. Oh-hashi, M. Higa, T. Matsui, T. Seo, H. Yanagisawa, and M. Tachiki, "A Method of Forming Null Beams for Arbitrary Array Antennas," in Proc. IEICE Spring Nat. Conv., vol.B, p.B-142, 1996.

N-STAR Ka-Band Antenna

*by Takao Itanami, Kenji Ueno, Izuru Naito and Yuji Kobayashi**

N-STAR[1] designates a series of Japanese domestic communications satellites of the NTT Group, Japan's privatized telephone and telegraph utility. They are multi-functional, providing S-, C-, Ku- and Ka-band services. Of the various antennas installed on them, this article summarizes the Ka-band antenna, which was developed by Mitsubishi Electric to be used for both multibeams and shaped beams in common for uplink (30GHz) and downlink (20GHz) bands.

Antenna Configuration

The Ka-band antenna is shown under test in Fig. 1. It is an array-fed offset Gregorian type with 2.2m-diameter aperture. A subreflector and feed arrays consisting of pyramidal horns are accommodated in a tower. This tower has a window that provides a path for the beams between the main reflector and the subreflector.

The major specifications of this antenna are shown in Table 1. It is multi-functional, generating multibeams and shaped beams simultaneously. The multibeams cover the whole of Japan (including the southernmost islands of Okinawa) with eight beams in the uplink band (30GHz) and three beams in the downlink band (20GHz). The shaped beams cover the Japanese mainland, that is, the four main islands of Honshu, Kyushu, Shikoku and Hokkaido with one beam each in uplink and downlink bands. Adequate sidelobe isolation between uplink multibeams is achieved for frequency reuse between every fourth beam, e.g., between the first and the fifth, the second and sixth, etc. There is no frequency reuse in downlink multibeams. Table 2 shows the frequency allocation for each beam of this antenna and Fig. 2 illustrates the multibeam coverage for uplinks.

In order to generate the variety of beams described, a curved frequency selective reflector (FSR) is employed as the subreflector to allow space diplexing for separate feeds between uplink and downlink beams. The subreflector is shown in Fig. 3, and the space-diplexing function it provides is illustrated in Fig.4. The subreflector has a double-wall construction consisting of the front curved FSR and the rear solid reflector. The front reflector consists of some 16,000 resonant elements photo-etched on the surface so as to be transparent to 30GHz-band uplink signals and to reflect 20GHz-band down-

Fig. 1 The Ka-Band Antenna Under Test.

Table 1 Major specifications of the Ka-band antenna

	Uplink		Downlink	
	Multibeam	Shaped	Multibeam	Shaped
No. of beams	8	1	3	1
Frequency	30GHz band		20GHz band	
Polarization	LH circular		RH circular	
Antenna type	2.2m-diam. offset Gregorian			

Table 2 Frequency allocation of Ka-band antenna

Uplink (30GHz band)									
Beam	Multibeam								Shaped
	#1	#2	#3	#4	#5	#6	#7	#8	
Freq.	f_1	f_2	f_3	f_4	f_1	f_2	f_3	f_4	27.0~28.2GHz
	28.3~30.4GHz								

Downlink (20GHz band)				
Beam		Multibeam		Shaped
	#1	#2	#3	
Freq.	f_5	f_6	f_7	17.8~18.4GHz
	18.5~20.1GHz			

**Takao Itanami is with NTT Service Integration Laboratories, Kenji Ueno is with Advanced Space Communications Research Laboratory, Izuru Naito is with Information Technology R&D Center and Yuji Kobayashi is with Kamakura Works.*

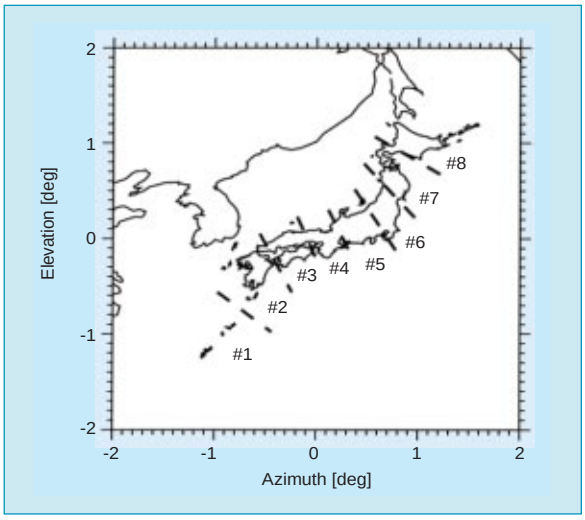

Fig. 2 Multibeam Coverage for Uplink (30GHz band).

Fig. 3 The Subreflector Assembly.

link signals. The quasi-periodic disposition of elements on the curved surface is made by the novel method developed.[2] Double-ring resonant elements with reduced polarization dependency are adopted for circular polarization applications in the Ka band. The curved front FSR and solid rear reflector are connected with ribs around the reflectors. The curved surfaces on the FSR and rear reflector are both ellipsoidal. One focus of each surface is common to the focus of the paraboloidal main reflector and the other foci of the front and rear reflectors are displaced from one another. This configuration allows for separation between uplink and downlink feed arrays.

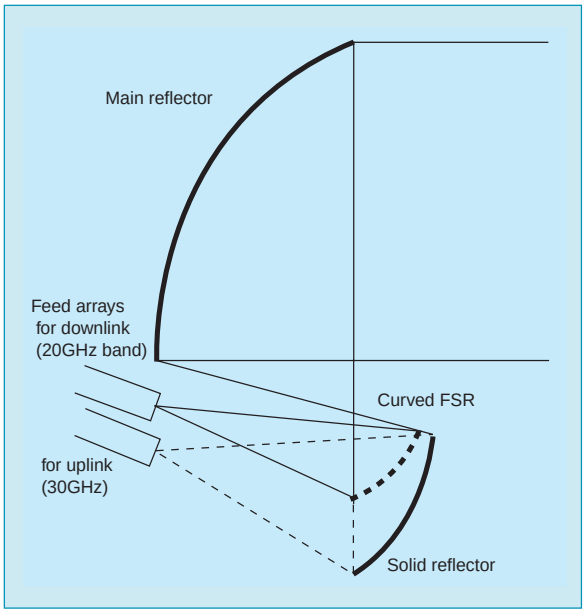

Fig. 4 Schematic Showing How the Double-Wall Subreflector (FSR and solid) Achieves the Space Diplexing Function.

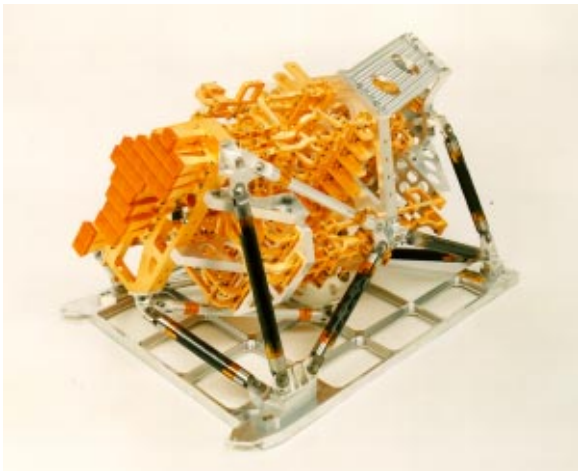

Fig. 5 Feed Array and BFN for Uplink (30GHz band).

Feed Arrays and Beam-Forming Networks

The feed array and beam-forming network (BFN) for uplink are shown in Fig.5. Those for download are similarly configured. The uplink feed array consists of 26 pyramidal horns and the downlink feed array of 14 pyramidal horns. Each horn is excited via waveguide BFNs. Both of the

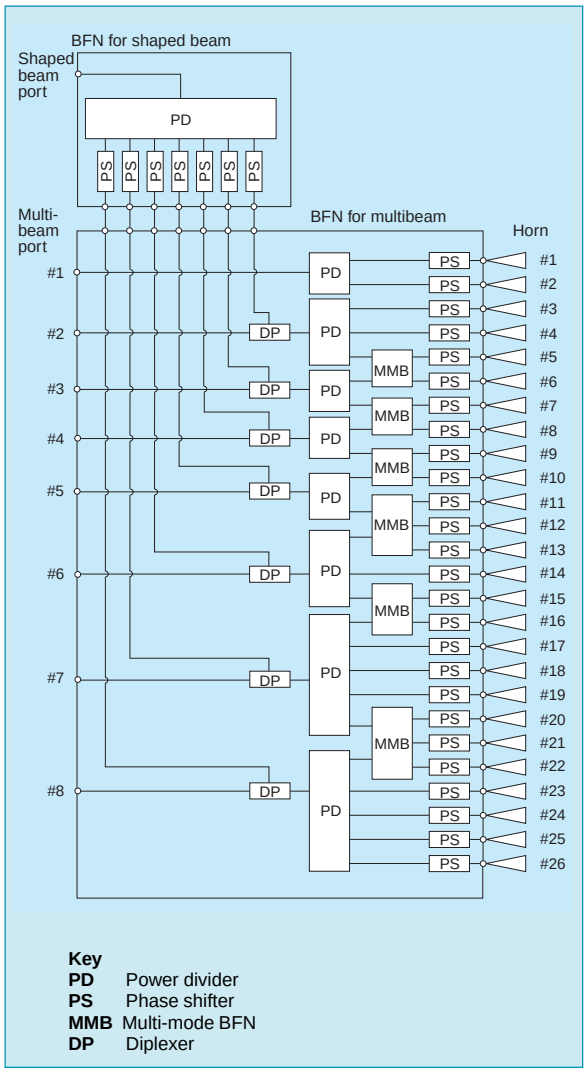

Fig. 6 Block Diagram of BFN for Uplink (30GHz band).

feed arrays for uplink and downlink are used in common for multibeams and shaped beams. The uplink feed array generates eight multibeams (two folded-frequency reuse) and one shaped beam, and the downlink feed array generates three multibeams (with no frequency reuse) and one shaped beam.

The block diagram of the BFNs for uplink is shown in Fig. 6. That for downlink is similar. BFNs are divided into two categories; those for multibeams and those for shaped beams. The former distribute signals to multiple horns for each multibeam, with some horns used in common by adjacent multibeams in order to provide continuous coverage of the whole land area of Japan. Common-use horns use multi-mode BFNs.[3] The multi-mode BFNs consist of hybrids and phase shifters, and have multiple input/output ports. Amplitude and phase at the output ports correspond to the input port selected and are determined by the parameters of the hybrids and phase shifters. The amplitude and phase values cannot be independently controlled for each input port. Therefore, unlike conventional BFNs, the BFNs for multi-mode multibeam connections must be designed specifically for each multibeam. A novel simultaneous design technique has been developed and applied to the BFNs for multibeams to achieve the appropriate horn-excitation coefficients.

The BFNs for shaped beams distribute signals to the midpoint of the BFNs for multibeams via diplexers. These shaped-beam BFNs are designed to achieve the desired amplitude and phase at the output ports connected to the diplexers. The desired amplitude and phase for the appropriate horn-excitation coefficients for shaped beams are derived by simulation. The simulation is rigorously performed using equivalent-circuit models corresponding to the hardware of the BFNs for multibeams and diplexers.

A number of novel techniques have contributed to the development of these flexible and efficient Ka-band antennas, which serve to provide reliable and continuous coverage of the entire land area of the Japanese archipelago. ❑

References

[1] Nakagawa, K., Minomo, M., Tanaka, M., Itanimi, T. : N-STAR: Communication satellite for Japanese domestic use, 14th AIAA International Communications Satellite Systems Conference, AIAA-94-1078-CP, pp.1129-1134 (1994).

[2] Itanami, T., Ueno, K., Honma, S., Noguchi, T., Makino, S., Ishida, O.: Arrangement methods of the resonators on a curved FSR, 1991 Autumn Nat. Conv. Rec. IEICE, B-25 (1991) (in Japanese).

[3] Patenaude, E., Amyotte, E., Ilott, P., Menard, F., Gupta, S., Mok, C.: MSAT L band antenna subsystems, 14th AIAA International Communications Satellite Systems Conference, AIAA-94-0984-CP, pp.449-567 (1994).

Adaptive Attitude Control of Spacecraft with Movable Antennas

*by Katsuhiko Yamada and Shoji Yoshikawa**

Studies on adaptive attitude control are underway to minimize satellite attitude disturbance associated with movement of large antenna assemblies. Parameter estimation accuracy has been improved by supplementing conventional attitude control laws with a simple online parameter estimation law. This enables a satellite antenna assembly to be moved rapidly while maintaining the satellite in a precise attitude.

Recent observation and data-relay satellites are being fitted with large movable antenna assemblies for interorbit (i.e. satellite-to-satellite) communications (Fig. 1). The action of a motor driving the antenna assembly to a new position creates a counter-torque that tends to rotate the satellite body, and the momentum of this rotation must be canceled through the operation of the satellite's thrusters and wheels driven by a feed-forward control loop. By using a momentum equation to calculate the effect of the antenna movement, the wheels can be driven simultaneously to cancel the unintended momentum. This method reduces attitude fluctuations without raising the feedback gain of the attitude-control system. A problem with this approach is that compensation is calculated by a numerical model of the momentum equation so the torque errors resulting from inaccuracies in the model are not canceled and tend to accumulate. The adaptive attitude control system presented here overcomes these problems of feed-forward control systems. Under this method, model errors are identified and measured by the attitude fluctuations that result and this information is used to compensate for model errors.

We will now examine the control system design and give examples of numerical simulation.

The following equation expresses the conservation of the system's angular momentum, which include components of the satellite and momentum. Note that the while the parameter estimation rule is operating the thrusters are providing no external force so that angular momentum remains constant.

$$M\dot{\boldsymbol{\theta}} + m\dot{\boldsymbol{\phi}} + \boldsymbol{w} = 0 \quad \text{..... (Eq. 1)}$$

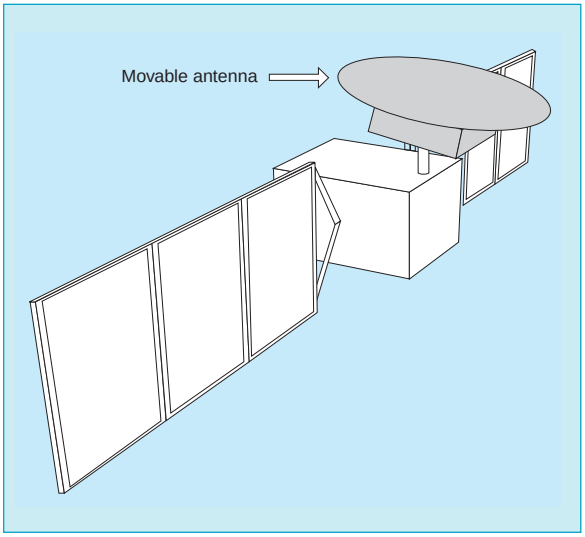

Fig. 1 Model of satellite with a large movable antenna.

$\boldsymbol{\theta}$, $\boldsymbol{\phi}$ and $\boldsymbol{w}$ are vectors representing the satellite attitude angle, the angle of antenna displacement and the wheels' angular momentum, respectively. M and m are the mass matrices for $\boldsymbol{\theta}$ and $\boldsymbol{\phi}$ and $m\dot{\boldsymbol{\phi}}$ is the angular momentum term created by the antenna movement, and expresses the satellite attitude fluctuation at satellite attitude angle $\boldsymbol{\theta}$. We can express $m\dot{\boldsymbol{\phi}}$ from the antenna rotation angle and antenna rotation speed, making it possible to separate constant parameters:

$$m\dot{\boldsymbol{\phi}} = \boldsymbol{Y}\boldsymbol{\alpha} \quad \text{.....(Eq. 2)}$$

$\boldsymbol{Y}$ is a matrix describing the antenna angle and angular velocity, and is known from the antenna rotation command. $\boldsymbol{\alpha}$ is a vector depending on the satellite and antenna mass, the position of the center of mass, and the moment of inertia. $\boldsymbol{\alpha}$ is not always known, but may be treated as a constant. The basic principle of online parameter estimation is using the linear relationship between the angular momentum of the attitude disturbance and $\boldsymbol{\alpha}$, a vector with unknown parameters. By simple inference, the estimated value for $\boldsymbol{\alpha}$ can be brought to converge on the true value.

**Katsuhiko Yamada and Shoji Yoshikawa are with the Advanced Technology R&D Center.*

If $\hat{\alpha}$ is the initial estimate for α, we can write the following attitude control law:

$$w = -Y\hat{\alpha} + K_P\theta + K_I\xi,\ \xi = \int\theta dt \quad \text{.....(Eq. 3)}$$

where w is the angular momentum command value, and K_P and K_I are the control gain. This is a classical proportional and differential control law (proportional and integral with respect to the wheel momentum) with a feed-forward control law added. Implementing local feedback on the wheel allows momentum commands to be given. Deriving w from Eq. 3, then pseudo differentiation gives us the wheel torque commands. In either case, the wheel achieves an angular momentum almost exactly as specified. Considering the change of $\hat{\alpha}$ over time, we add the following parameter estimation law.

$$\dot{\hat{\alpha}} = -PY^T\theta \quad \text{.....(Eq. 4)}$$

where P is a symmetric positive definite estimated gain matrix. This parameter estimation law is taken from adaptive control laws for ground-based manipulators, but in a simplified form because it is based on the conservation of angular momentum expressed in Eq. 1. The adaptive attitude control law we are proposing here is a conventional attitude control law with the parameter estimation law of Eq. 4. The stability of this control law can be established by the Lyapunov function, showing that the attitude angle converges to zero. By adding a simple parameter estimation law (Eq. 4) to a conventional attitude control law with feed forward (Eq. 3), the attitude control error approaches zero even when an estimation error occurs. Analyzing the behavior of the approach of the parameter estimation value $\hat{\alpha}$, we can show that $\hat{\alpha}$ approaches the true value of α.

Fig. 2 shows a block diagram of the control system. Except for the point where the parameter estimation law causes $\hat{\alpha}$ to fluctuate, behavior is similar to conventional attitude control systems. The $\hat{\alpha}$ used in the parameter estimation law need not include all the components of α, and in fact, it is better to choose only the most influential components. As for the other components, by using an initial estimate, the parameter estimation law (Eq. 4) is simplified. When the parameter estimation law has been used to estimate the parameters, even returning to a conventional attitude control law, the unknown parameters approach the true values,

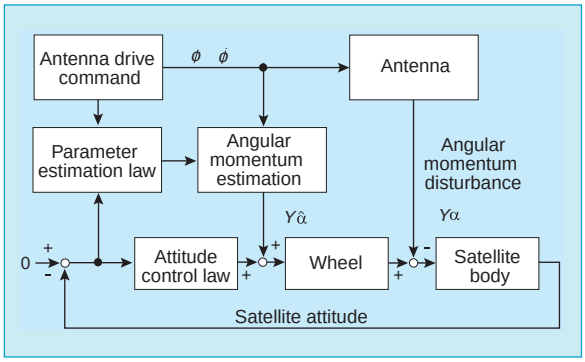

Fig. 2 Block diagram of adaptive attitude control system.

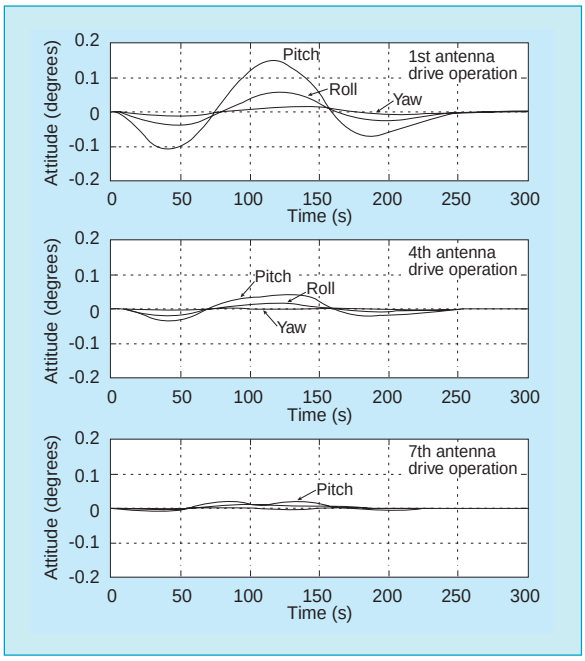

Fig. 3 Attitude variation during first, fourth and seventh antenna drive operations. The initial values of the estimated parameters are 80% of the true parameter value.

and the attitude control precision improvement remains. That is, estimating online parameters at the start of antenna operation results in improved attitude control precision when the antenna is operated.

We will now describe the simulation of a satellite with a movable antenna as shown in Fig. 1 that was conducted to verify the adaptive satellite attitude control law. The antenna was moved 20° back and forth and this cycle was repeated to determine the cumulative effect on satellite attitude error. Fig. 3 shows the effect of antenna movements on satellite attitude fluctuations on the 1st, 4th and 7th movement when the initial value of the estimated parameter $\hat{\alpha}$ is 80% of the true value α. As the antenna is moved more times, the estimate accuracy increases, so that even fast antenna movements can be absorbed by wheel movements, leading to high attitude precision.

Because the bandwidth of the attitude control is narrow due to structural flexibility, attitude error increases during the antenna motion, disturbing the stability required for effective communications. This problem is heightened as satellites are fitted with large, movable antenna assemblies that apply torques to the satellites when they are moved. By feeding attitude errors back into the control equation to improve parameter estimation, it becomes possible to effectively damp these disturbances. ❑

Digital Circuit Multiplication Equipment Based on Intelsat Specifications

*by Nobuhiro Gencho and Mitsuhiro Takemoto**

Mitsubishi Electric has developed Model DX-5000 digital circuit multiplication equipment (DCME) based on the Intelsat IESS-501 Revision 3 specifications. Field tests for the equipment were completed and commercial deliveries began in May 1995.

DCME uses three essential techniques: digital speech interpolation, ADPCM and fax demodulation and transmission technologies. DCME is generally installed between an international switching center (ISC) exchange and a satellite earth station transceiver (Fig. 1).

IESS-501 Revision 3 was drafted by Intelsat to ensure compatibility among DCME equipment from differing manufacturers, and the corporation's Model DX-5000 (Fig. 2) is fully compliant with its provisions. This article introduces the DX-5000 DCME and the results of its field testing.

Fig. 2 Model DX-5000.

Product Features

The DX-5000 achieves a gain of five by combining digital speech interpolation (DSI) technique with an ITU-T G.726 compliant ADPCM codec. The statistics for typical telephone conversations show that speech is present on each transmission line for only about 40% of the time. DSI operation dynamically connects the active trunk channels with the available bearer channels to achieve a multiplication factor, known as the DSI gain, of about 2.5.

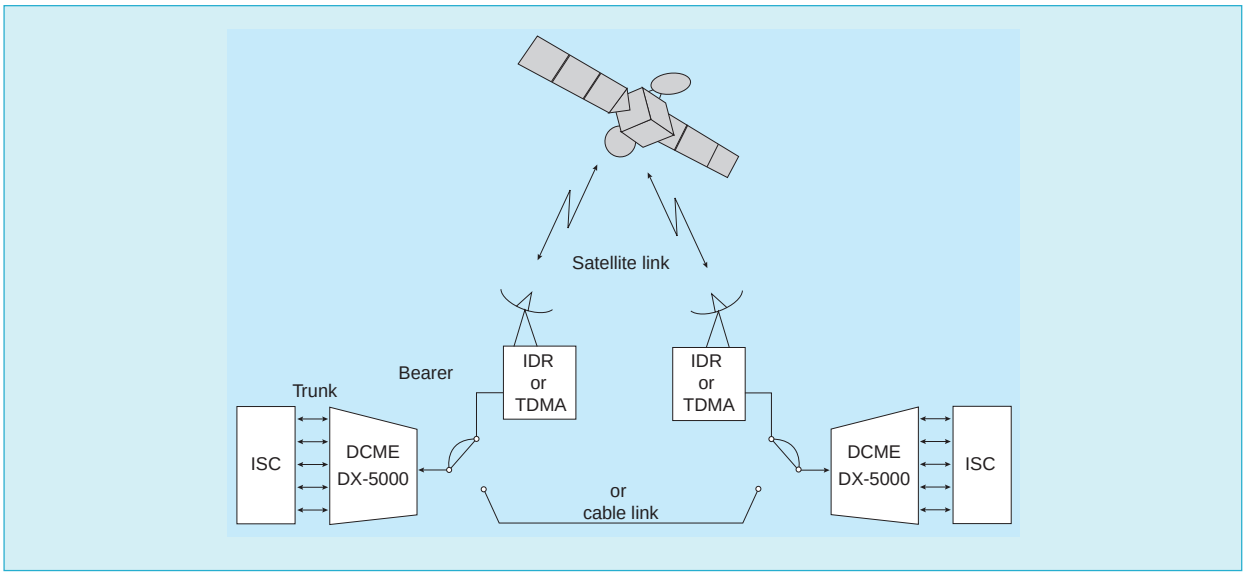

Fig. 1 Single destination topology.

**Nobuhiro Gencho and Mitsuhiro Takemoto are with the Communication Systems Center.*

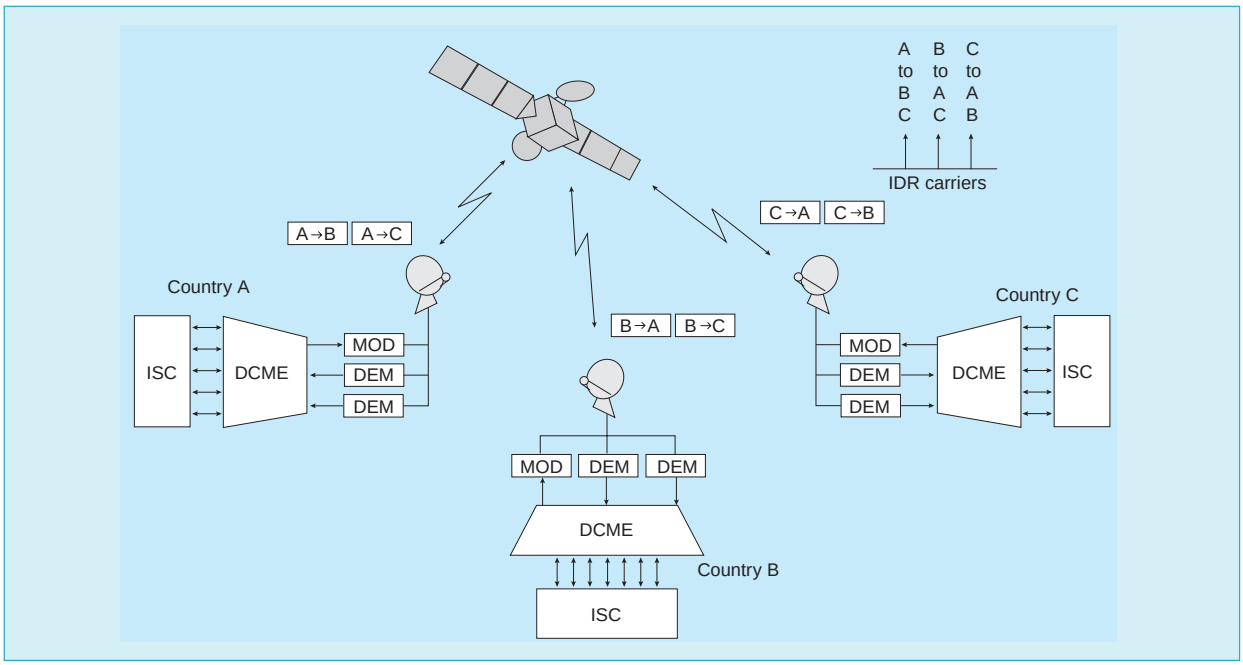

Fig. 3 Multiple clique topology.

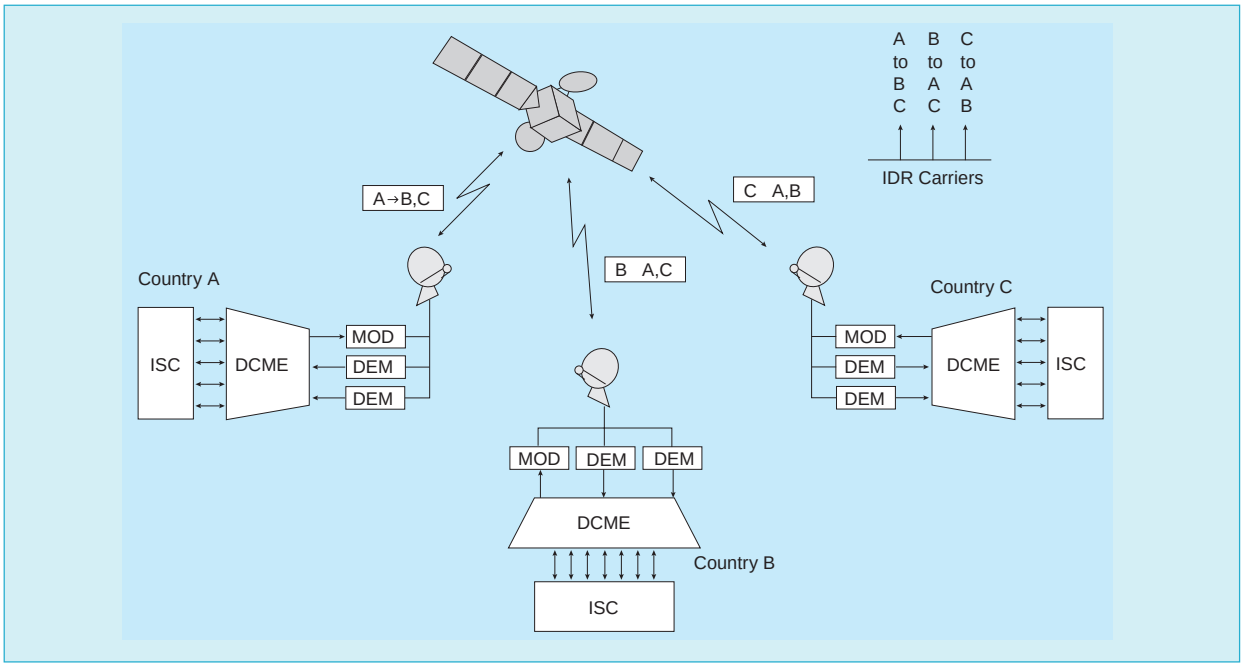

Fig. 4 Multiple destination topology.

The number of fax modems accommodated can be expanded up to 128 depending on the actual percentage of facsimiles in the traffic.

The DX-5000 has self-diagnostic functions. The customer can execute self-checking of fax modems and ADPCM codecs, and provides for transmission tests using bearer loopback. A single OMC console supports up to 80 DCME systems to collect alarm/event data, management statistical data and monitoring data.

Several network operations are supported: a point-to-point configuration (Fig. 1) a multiple clique configuration (Fig. 3) and a multiple destination configuration (Fig. 4).

The DX-5000 supports N:1 redundancy configuration; up to seven DCME terminals can be backed up by one redundant DCME terminal and are automatically switchable.

The G.726 ADPCM codec dynamically matches the transmission rate to the line load, with a

Table 1 Model DX-5000 Specifications

Interfaces	2.048Mbps CEPT, 1.544Mpbs T1
Operation modes	Single destination mode, multiple clique mode up to two destinations, multiple destination mode up to four destinations
No. of trunk channels	Up to 216 channels per trunk, up to 10 2.048Mbps trunks or 10 1.544Mbps trunks
No. of bearer channels	Up to 31 2.048Mbps channels or 24 1.544Mbps channels
No. of voice bearer channels	
2.048Mbps bearer	122 channels max, including 61 overload channels
1.544Mbps bearer	94 channels max, including 47 overload channels
DSI processing	5/4/3/2 bit mode operation
Channel usage configuration	16/24/32/40kbps DSI, 32/40kbps DNI or 64kbps clear channel
Signaling	ITU-T Nos. 5, 6, 7, R1, R2
Q.50 functions	ITU-T Q.50 Annex A, B
Data transfer	Rates up to 9600bps guaranteed through 40kbps ADPCM coding
Demodulated fax data	Up to 128 sets
Fax demodulation signal	
Type	ITU-T T.30 standard protocol, GIII facsimile signal
Data rates	
V.17	7,200, 9,600, 12,000 and 14,400bps
V.29	7,200 and 9,600bps
V.27	2,400 and 4,800bps
V.21	300bps
ADPCM codec	ITU-T G.726
Rack dimensions	2,100 x 650 x 450mm (H x W x D)
Power consumption	300W
DX-5000 panel	445 x 552 x 370mm (H x W x D)
DX-5000 weight	60kg

maximum rate of 16kbps. The DX-5000 can demodulate and remodulate modem signals up to V.17/14.4kbps for GIII standard facsimile transmission.

Table 1 lists the major specifications, which are derived from IESS-501 Revision 3, ITU-T G.763 and G.766.

Field Testing Results

Testing began in March 1993 at the Intelsat Technical Laboratory in the United States. Drafted by Intelsat, the test program included 143 items covering transmission of fax, tone and voice signals and other items to establish interoperability with other manufacturers' DCME systems. All test items were completed by the March 1996 deadline, then field testing was conducted pairing the Mitsubishi DCME with equipment from the Israeli manufacturer ECI. The following paragraphs describe field tests conducted in May 1996 over a Canada-to-Sweden link under Intelsat guidance.

The tests were conducted over a 2.048Mbps IDR network system with two Mitsubishi Electric DX-5000 DCME units installed in Sweden and two DTX-360 units from ECI installed in Canada.

The tests were divided into three phases: confirming proper equipment operation by each manufacturer's engineers, performance measurements over the satellite link, and finally live traffic tests over the link.

In the initial operational tests, simulated tone signals, simulated 9.6kbps voice-band data signals or simulated voice signals were sent over the trunk and statistical data were monitored at the OMC console. In fax transmission tests, two types of fax simulator and some real fax machines which supported actual V.17/14.4kbps and V.29/9.6kbps transmission were used. V.34/28.8kbps modems were also tested, and the the modem signal was transmitted at the 19.2kbps data rate.

In the next stage of testing, simulated voice, simulated voice-band data and fax signals were transmitted simultaneously and statistical data were analyzed to check for problems.

In the final stage of testing, engineers from Intelsat and Sweden's Telia Corporation verified that the DCME equipment functioned properly when carrying actual signal traffic. These tests found no interoperability problems.

Advanced functionality such as variable-rate codecs and dynamic speech interpolation improve the efficiency of Mitsubishi DX-5000 DCME equipment, maximizing utilization of satellite communications capacity. ❑

A Digital Satellite Newsgathering System

*by Masamizu Hinata and Tatsuhiro Oba**

MPEG2-based digital video technologies are being incorporated into satellite newsgathering (SNG) systems to lower broadcasters' sound and video signal transmission costs. Mitsubishi Electric has recently developed eight-phase digital phase-shift keying (PSK) modulation technologies and video bandwidth compression technologies that enable a single satellite transponder to carry four video channels—double the two-channel capacity of the previously used analog FM modulation system—while boosting video image quality. In addition, a demand assignment multiple access (DAMA) system has been developed to use excess transponder capacity for emergency communications. All data transmissions, including order wire signals, have been converted to digital form.

Commercial domestic satellite communication services began in Japan in 1989 with the launch of private-sector communication satellites. Satellite links were soon employed for broadcast network SNG systems, which benefit from the wide bandwidth, wide area coverage, minimal transmission delay and immunity to ground disturbances that distinguish satellite communications from terrestrial networks. The transmission costs of these first-generation SNG systems were high because the two-channel-per-transponder capacity available with the analog FM modulation system meant that a busy broadcast network would need more than one transponder to serve the needs of both newsgathering and relaying program content between stations. The development of eight-phase

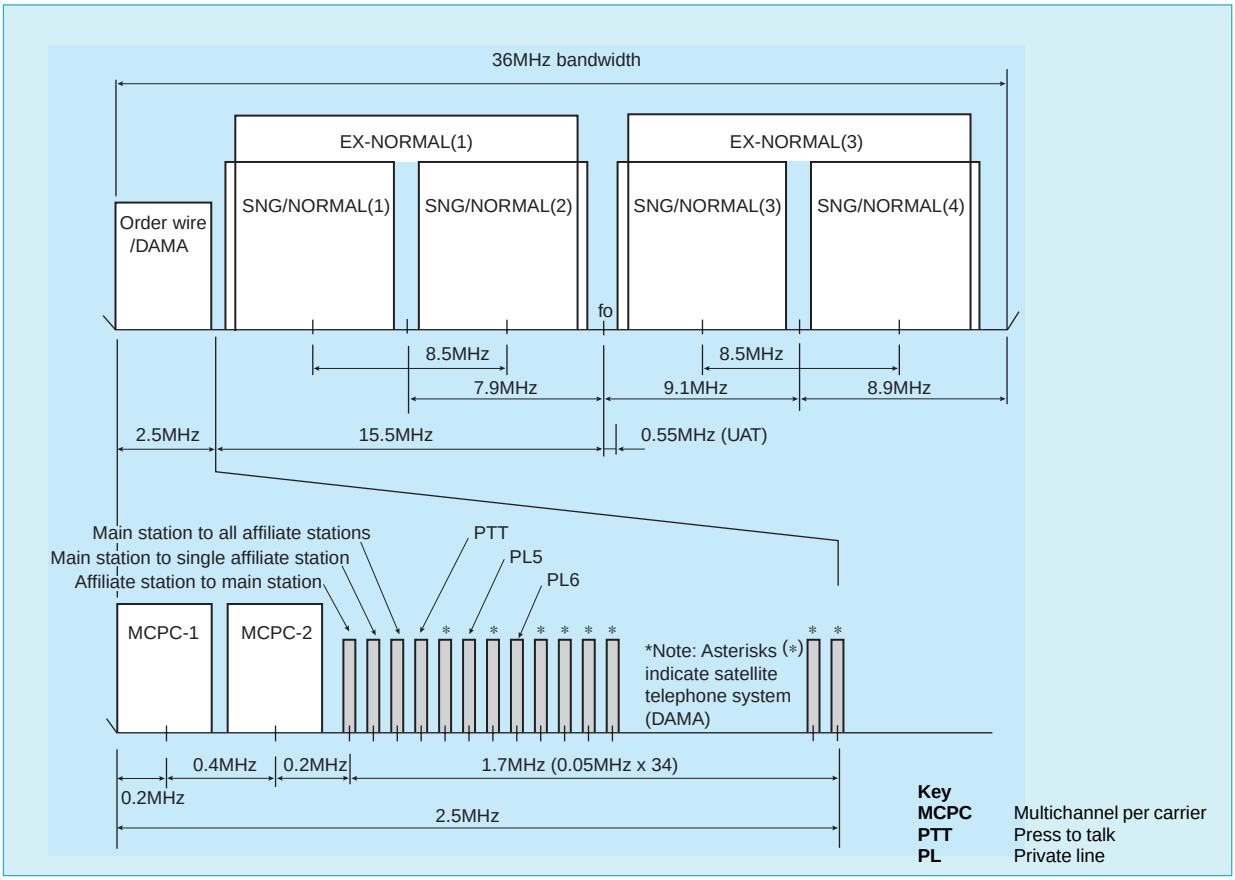

Fig. 1 The FSAT transponder frequency allocation.

**Masamizu Hinata and Tatsuhiro Oba are with the Communication Systems Center.*

PSK modulation systems ameliorates this problem by halving the bandwidth requirement for video and audio signal transmission.

Mitsubishi Electric's digital video codec, which is responsible for this increased capacity, uses discrete cosine transform (DCT) movement prediction to achieve high coding efficiency. Two types of modulation are supported. QPSK modulation with two levels of error correction (convolutional coding with Viterbi decoding and Reed-Solomon coding/decoding) provides robustness and a lower operation rate for use in rain or other adverse conditions. Eight-phase PSK modulation is available to support higher operation rates permitting high-quality images to be carried at half the transmission cost per channel.

Network Configuration

Mitsubishi Electric is working with Fuji Television, which serves as the main network hub, along with Kansai Television and other affiliated broadcasters to build FSAT, a digital network that will eventually link 26 stations. The network will use multiple flexibly configured channels that will reduce transmission costs. Increased rate of operation and reduced cross-channel interference will improve picture quality, while data scrambling will protect these signals against unauthorized reception. The equipment size is being reduced to save space in mobile satellite trucks.

The channel configuration and picture quality goals are realized by the frequency allocation scheme illustrated in Fig. 1. The system operates in a two-channel EX-NORMAL mode, and in a four-channel NORMAL/SNG mode.

Video Codec

The video encoder includes digital audio and video coding units that compress the signal bandwidth. The compressed digital signal is then

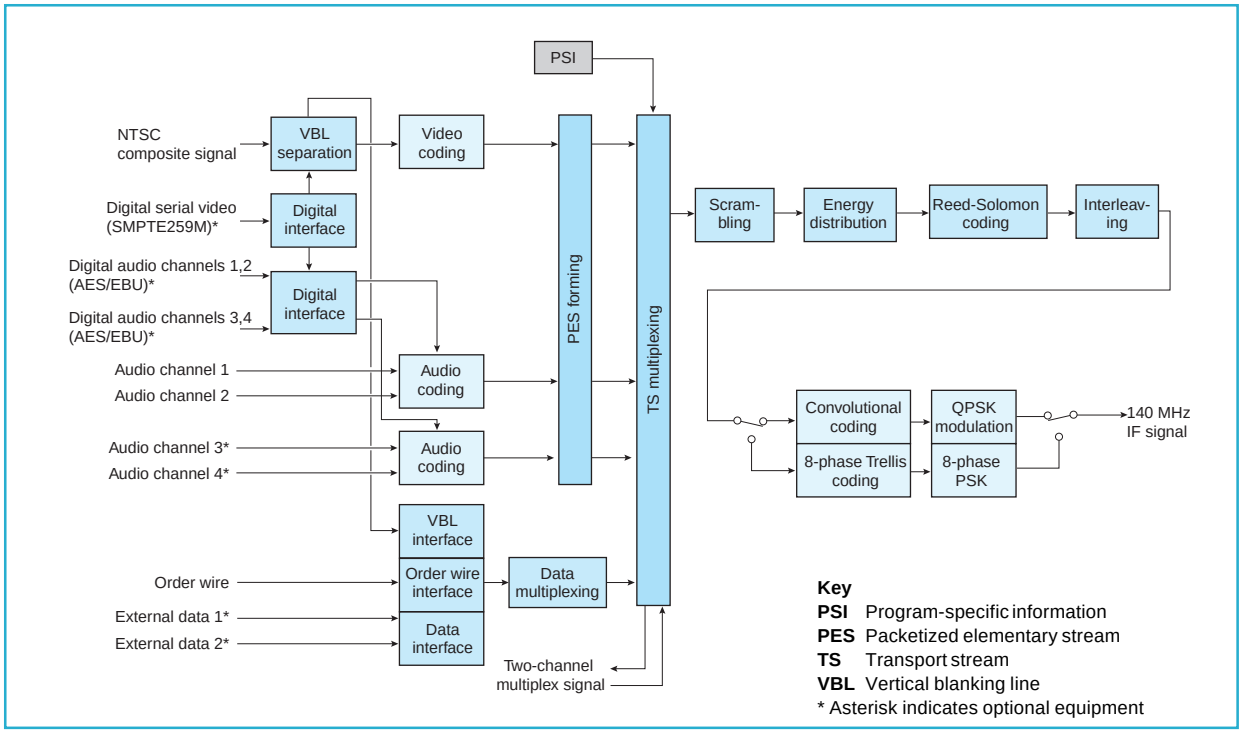

Fig. 2 Block diagram of Model VX-3000E video encoder equipment.

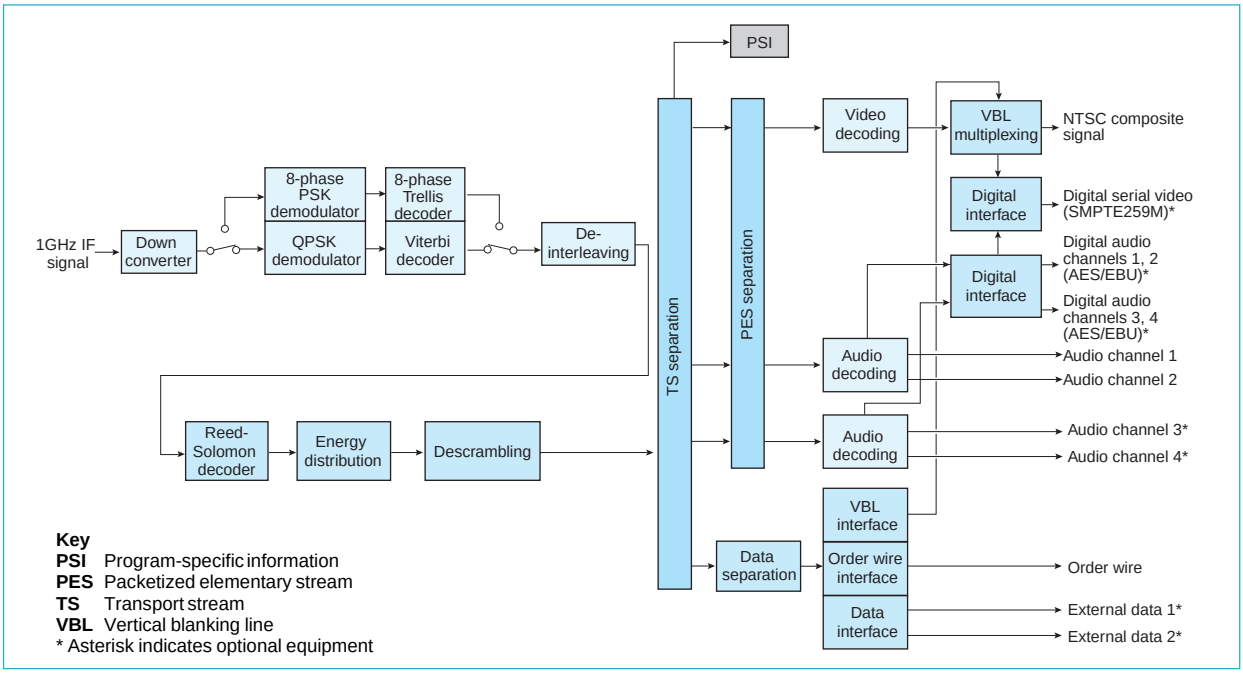

Fig. 3 Block diagram of Model VX-3000D video decoder equipment.

packetized, forming what is called a packetized elementary stream (PES). The video blanking line signal is separated and multiplexed with the order wire signal. The PES and order wire signals are then multiplexed to form a transport stream (TS). The transport stream is then scrambled for privacy and energy distribution purposes, and Reed-Solomon coding is applied. After interleaving, convolutional coding is used for QPSK modulation and Trellis coding for eight-phase PSK. Finally, digital modulation is performed in an orthogonal modulator, yielding a 140MHz intermediate frequency (IF) signal output.

The video decoder performs frequency conversion on the received 1GHz IF signal followed by demodulation by coherent detection. Viterbi decoding is used for QPSK signals and TCM decoding for eight-phase PSK in a reversal of the coding process to recover and separate the original video, audio and order-wire signals.

Fig. 2 shows a block diagram of video encoder Model VX-3000E and Fig. 3 a block diagram of video decoder Model VX-3000D. The basic features of this equipment are as follows: MPEG2 compliance, four- and eight-phase operating modes, various transmission modes, digital video interface functions, order wire support, net queue signals multiplexed with vertical blanking line signals, and signal scrambling support.

The digital SNG system described here has been implemented, tested, and found to reduce cross-channel interference to levels well below that of previous analog FM, boosting picture quality even while transmitting four video channels. At the same time, the ability to transmit four channels per transponder has halved signal transmission costs. The authors would like to thank Fuji Television and its affiliates for cooperation that has been instrumental in assembling the FSAT network. ❑

Automatic Rendezvous and Docking Experiments

*by Hiroshi Koyama and Makoto Kunugi**

The world's first successful rendezvous and docking between unmanned spacecraft was achieved on July 7, 1998, between two ETS-VII satellites. Thrustering problems that arose during a second experiment a month later were eventually resolved and a second docking achieved on August 27.

The two ETS-VII satellites—*Orihime* the target and *Hikoboshi* the chaser—were launched in November 1997 aboard an H-II rocket, and orbited while coupled together at an altitude of 550km.

Working under Japan's National Space Development Agency (NASDA), Mitsubishi Electric oversaw development of the rendezvous and docking system and the ground operation system and continues to work with NASDA on preparations and operations support for ongoing on-orbit experiments. The navigation, guidance and control system was researched, designed and tested by Mitsubishi Electric. The company conducted closed loop tests of the assembled hardware and software and other ground-based testing to qualify the systems for flight.

Once the satellites were in orbit, the company also tested the rendezvous-related functions of the navigation, guidance and control system prior to the first on-orbit docking attempt.

The first test was designed to evaluate the on-orbit performance of the docking and separation systems and the navigation, guidance and control systems at separations under 2m. On July 7 at 7:09am, operators using a special control console at the Tsukuba Space Center sent a command to *Hikoboshi* to decouple and push the two spacecraft apart at a rate of about 2cm/s. After separation, an image sensor aboard chaser *Hikoboshi* extracted information about the relative position and attitude of the satellites. This information was used by a control system that simultaneously manages the relative position and attitude of the satellites—six axes in all—to maintain a constant relative attitude and position. A separation of about 2m was sustained for about 15 minutes. Then a command from the ground was sent to initiate a final approach using a rendezvous control function in which the chaser satellite squares to the target satellite prior to docking. *Hikoboshi* approached *Orihime* at about 1cm/s, captured the target's docking mechanism and completed docking at 7:33am.

Fig. 1 shows the relative attitude and position data (six axes) for the

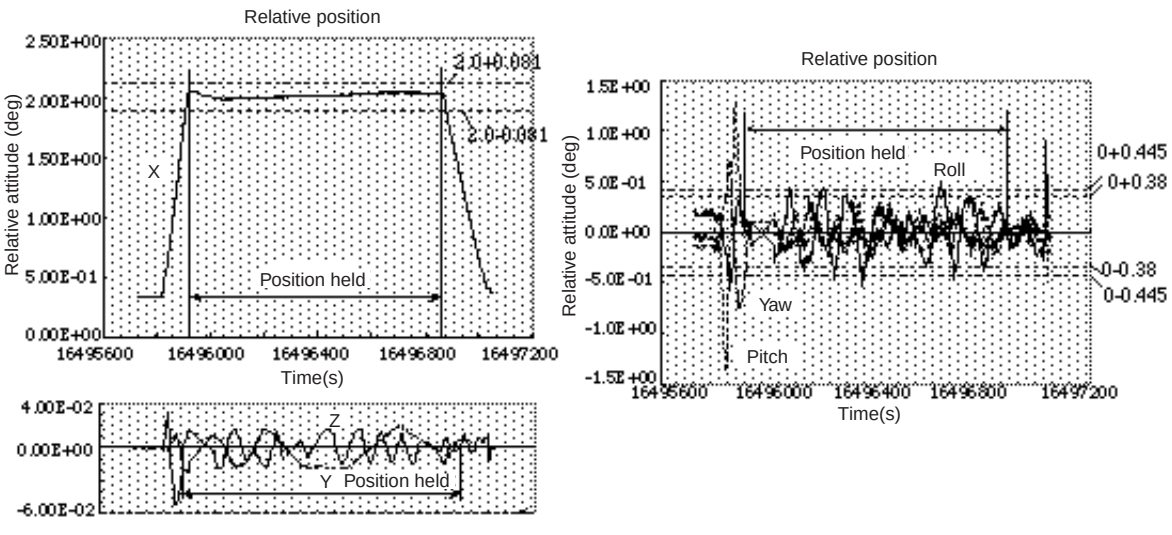

Fig. 1 Docking position and attitude data plotted with respect to time.

**Hiroshi Koyama and Makoto Kunugi are with the Kamakura Works.*

experiments. Fig. 2 shows a photo of the docked condition. The upper part of the docking mechanism belongs to *Orihime*, the lower part to *Hikoboshi*.

The second rendezvous and docking experiment was conducted at a separation of 500m to evaluate the in-flight performance of the navigation, guidance and control functions. The satellites separated on August 7 at 2:46am. The satellites were halted at the distance of 2m as in the previous test, and a chaser satellite pointing system using a laser-based rendezvous radar was switched on. After control switching, a command from the ground was to send *Hikoboshi* back at a speed of 10cm/s to a distance of 520m. Fig. 3 shows a photograph of *Orihime* taken from *Hikoboshi* after separation. After confirming that *Hikoboshi* had stopped at 520m, ground control sent a command to approach *Orihime*. Ordinarily, *Hikoboshi*'s control system ensures that the satellite faces *Orihime*, but an attitude control problem arose during the final approach forcing the system to enter a fail-safe mode designed to minimize risk of a collision. Engineers on the ground determined that a momentary failure of *Hikoboshi*'s propulsion system was responsible. Various thrust levels were tried in an attempt to work around the irregularity but the attitude control problems continued and the docking attempt was eventually aborted.

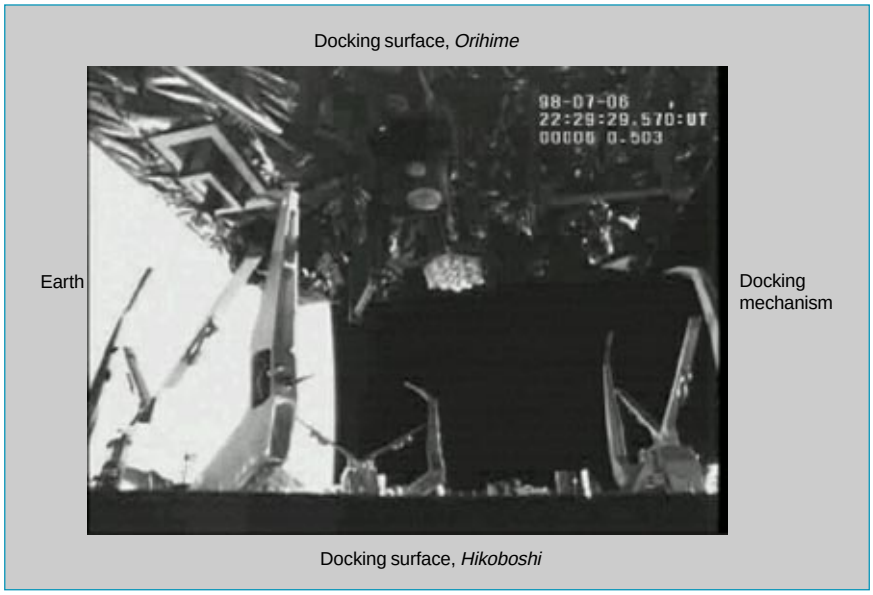

Fig. 2 A photo of the docked condition (courtesy of NASDA).

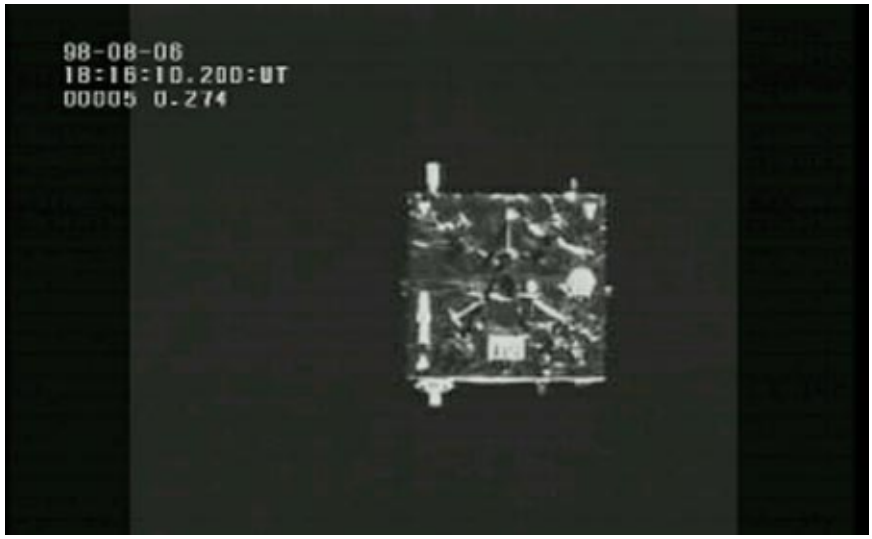

Fig. 3 A photo of Orihime *from* Hikoboshi *(courtesy of NASDA).*

These problems were eventually overcome by developing new docking software that minimized reliance on the problem thruster. Also incorporated into the program were halt and resume functions that respond to a thruster problem by halting the approach, reestablishing attitude control, and then continuing the approach. The next docking attempt, conducted at 10:43pm on August 27, succeeded.

The mission featured extensive safety functions and utilization of a GPS-based relative navigation system for trajectory control that is the first of its kind. The satellites' rendezvous capabilities exceeded expectations, important flight data was gained and invaluable lessons learned. A study on the irregularities that occurred is continuing and the results will be reflected in future rendezvous and docking systems.

NASDA has contracted with Mitsubishi Electric to develop technologies for the H-II transfer vehicle (HTV) that Japan is developing to deliver resources to the International Space Station planned for launch in 2002. The supply spacecraft will use rendezvous and docking technologies based on the experiments described here. ❑

A Very Small Aperture Terminal

*by Shuji Nishimura and Seiya Inoue**

Mitsubishi Electric has developed a 30kg portable VSAT terminal that is easy to transport and set up, and supports voice, facsimile and data transmission. Weighing less than 4kg, the system's indoor unit is compact and easily transported.

The terminal consists of a 75cm offset parabola antenna, an outdoor unit and an indoor unit. Fig. 1 shows a photo of the system and Fig. 2 a block diagram. Table 1 lists the general specifications, Table 2 gives details of the indoor unit. The antenna, the antenna tripod and the support for the outdoor unit separate to facilitate transport and can be assembled without tools. Each piece weighs under 10kg.

Fig. 1 The complete VSAT terminal.

The outdoor unit consists of two functional blocks. The high-power converter (HPC) receives an intermediate frequency (IF) signal for transmission from the indoor unit, performs frequency conversion, amplifies the signal and delivers it to the antenna. The low-noise block converter (LNB) passes signals received by the antenna from a satellite through a low-noise amplifier and extracts the IF signal.

The indoor unit has a voice interface unit, a microprocessor that controls the system and modulator and demodulator circuits. It is fitted with connectors for a telephone handset, fax machine or synchronous or asynchronous modem. The outdoor unit and indoor unit are connected by two coaxial cables, one for transmitted signals, the other for received signals. The transmission cable also carries power for the outdoor unit, reference signals and monitoring and control signals.

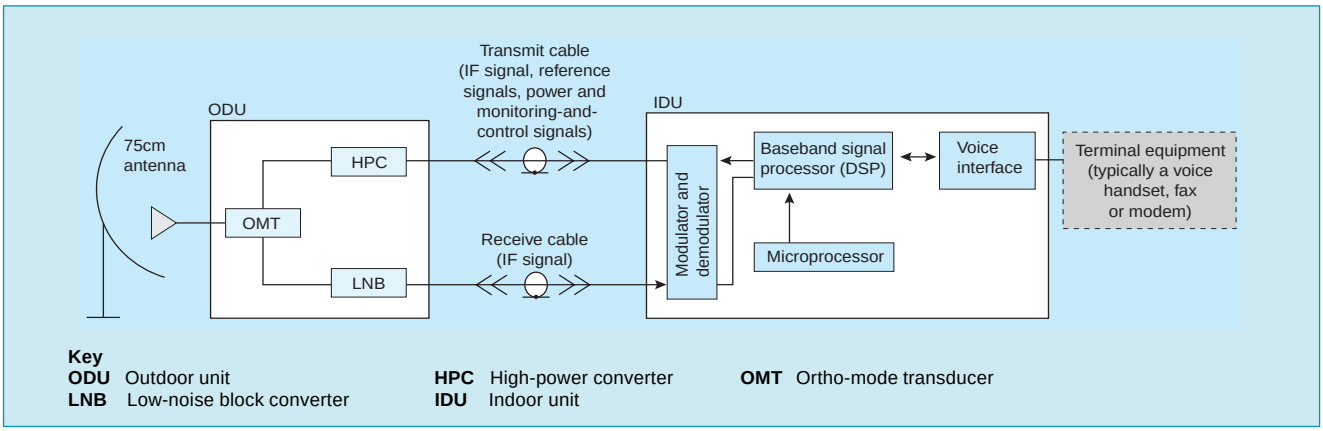

Fig. 2 A block diagram.

**Shuji Nishimura and Seiya Inoue are with the Communication Systems Center.*

Table 1 Main Specifications

Carrier frequency range	
Transmit	14 ~14.5GHz
Receive	12.25 ~12.75GHz
Intermediate frequency range	
Transmit	977~1,053MHz, 25kHz steps
Receive	950~1,450MHz, 25kHz steps
Antenna	75cm offset parabola
Transmit gain	Better than 38.7dBi at 14.25GHz
Receive gain	Better than 37.6dBi at 12.50GHz
Polarization	Linear, V/H or H/V
Weight	Under 17kg
Outdoor unit	
Transmit saturation power	1 or 2 watts
Receive noise temperature	170K max at 25°C
Weight	Under 8kg
Indoor unit	
Modulation method	QPSK
Voice coding	16kbps LD-CELP or 32kbps ADPCM
Frequency step size	25kHz
Input power	85~132VAC, 47~63Hz or 10~16VDC
Power dissipation	50W
Dimensions	330 x 263 x 86mm
Weight	Under 4kg
Operating environment	
Wind	Operates under gusts to 20m/s
Temperature, antenna & outdoor unit	–30 ~ +45°C
Temperature, indoor unit	0 ~ +40°C

Features

The weight of the indoor unit has been reduced, bringing the terminal's total weight to under 30kg. The terminal supports voice, facsimile and data communications. A second channel can be easily added to support simultaneous voice/fax or voice/data communications. The terminal is easily adapted to both demand assignment multiple access (DAMA) and preassignment multiple access (PAMA) line management protocols. Power for the system is supplied to the indoor unit: either a 12V car battery or an AC adapter plugged into a 100VAC supply may be used, with battery power permitting mobile or emergency use.

The Indoor Unit

Table 2 lists the major specifications of the indoor unit. The transmitter circuitry takes a voice-band signal from a handset, facsimile or modem, encodes the signal using quadrature shift phase keying (QPSK) modulation, and passes it to the outdoor unit. The receiver circuitry converts the frequency of the IF signal from the outdoor unit, applies coherent detection and extracts a baseband signal that is processed to demodulate the original voice signal. Volume and weight have both been reduced by a factor of four compared with the company's previous products. Weighing just 4kg, the unit is compact and lightweight, through use of direct modulation, a DSP baseband signal processor and simplified construction. A direct digital synthesizer using a phase-locked loop permits small IF frequency steps with low phase noise. Voice encoding by ITU-TG.728-compliant 16kbps low-delay code-excited linear prediction (LD-CELP) provides a narrow-bandwidth voice signal for effective bandwidth utilization. The system can also be switched to 32kbps adaptive differential pulse-code modulation (ADPCM) for compatibility with the company's previous terminals.

Baseband Signal Processor

The transmitter receives a voice signal from the voice interface, superimposes control signals received from the microprocessor and scrambles the result in one-frame units. Convolutional encoding is performed, followed by unique word multiplexing and Nyquist filtering. The signal is then delivered to the modulator.

Table 2 Indoor Unit Specifications

Modulation method	QPSK
Transmission rate	35kbps or 70kbps
Voice coding	16kbps LD-CELP or 32kbps ADPCM
Forward error correction	Convolutional coding R = 1/2 K = 7 with 3-bit soft-decision Viterbi decoding
Bit error rate	1 x 10^{-6} at Eb/No = 5.9dB
Multiple access protocol	DAMA or PAMA
User interface	
Voice	2- or 4-wire
Fax	G3 up to 9,600bps
Synchronous data	16kbps or 32kbps, RS232C or RS422
Asynchronous data	1,200~14,400bps, 28,800bps, RS232C

The receiver takes the baseband signal from the demodulator and performs quasicoherent detection with soft decisions to recover the encoded data. Unique word detection is used to establish a frame-synchronous reference that is used in subsequent Viterbi decoding and descrambling to deliver voice and control signals.

Modulator and Demodulator

The transmitter employs QPSK, a direct modulation method, in the 1GHz band. The receiver performs a single frequency conversion to extract the IF signal. The signal for one IF channel is selected and passed through an AGC to equalize the signal level. Detection is performed by the demodulator IC to recover the baseband signal.

Continued advancement in circuit integration combined with other power and weight-saving innovations have made this VSAT terminal power-efficient and easily transportable. ❑

A Notebook-Size Satellite Terminal

by Katsumi Tsukamoto and Atsushi Manzaki

Mitsubishi Electric has supplied terminal equipment for the MSAT mobile satellite communication system since 1995, when the geostationary satellite based service was inaugurated by American Mobile Satellite Corporation and TMI Communications. Mitsubishi Electric has previously supplied vehicle-mounted, transportable, marine and fixed-station MSAT terminals and has now developed OmniQuest, a notebook-size portable MSAT terminal. The OmniQuest terminal has a volume of about three liters and a weight of 2.4kg, approximately one fifth the volume and weight of the corporation's previous compact terminal equipment.

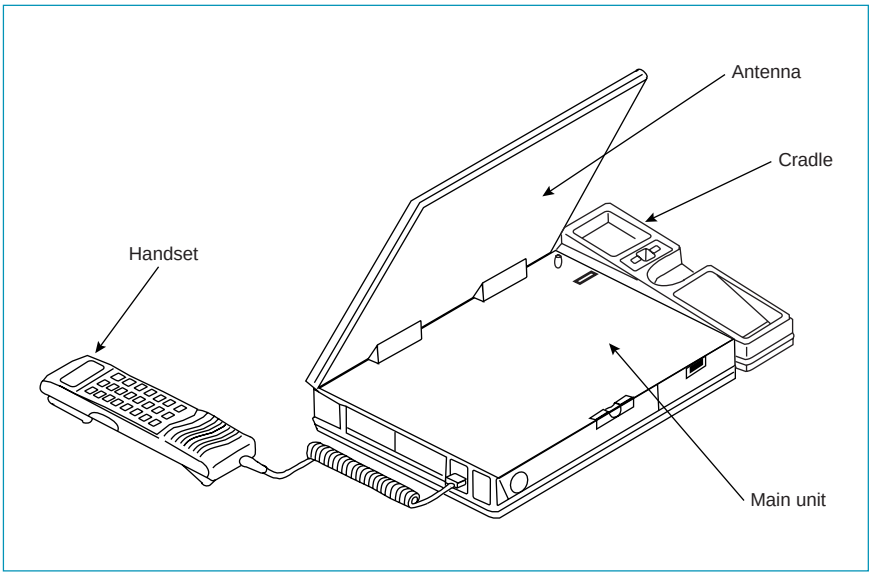

Fig. 1 The OmniQuest satellite terminal.

As with the corporation's previous MSAT terminals, OmniQuest supports voice, data, facsimile and dispatch radio services. The battery operating time, a key parameter of portable equipment, is one hour of continuous transmission or eight hours on standby. This report describes the size reductions achieved through technical advances including a thin antenna, compact RF and digital signal processing circuitry and reduced power consumption. Compact dimensions and light weight make the product suitable for personal as well as business use.

Fig. 1 shows an illustration of the terminal and Fig. 2 a block diagram. When the terminal is used, a lid containing the antenna is opened

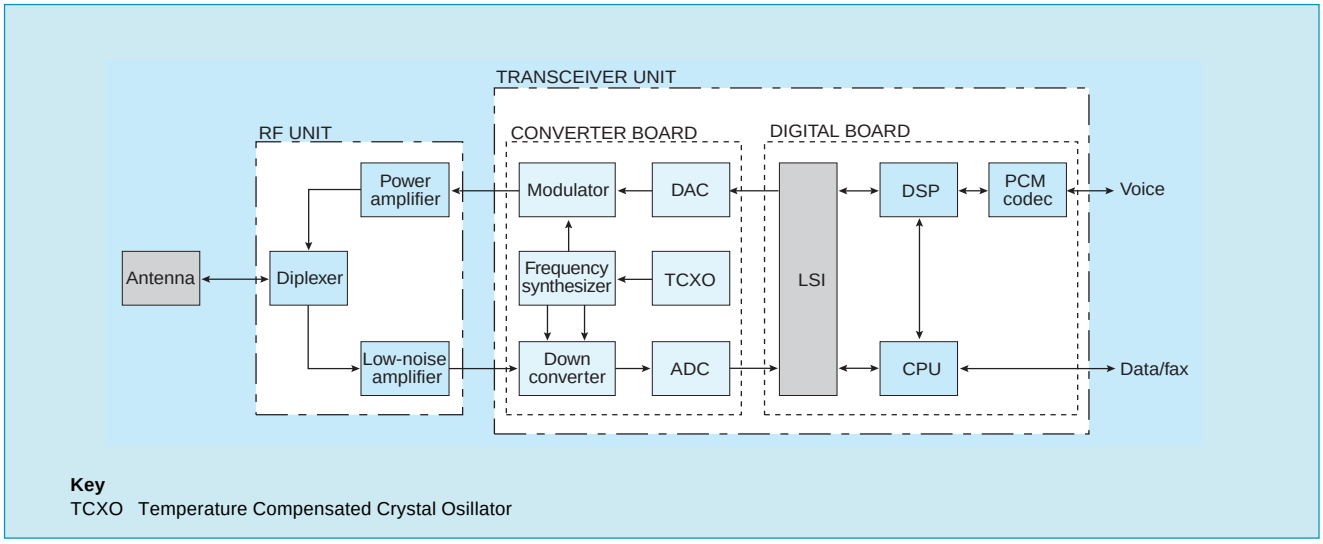

Fig. 2 A block diagram of the OmniQuest terminal.

*Katsumi Tsukamoto and Atsushi Manzaki are with the Communication Systems Center.

Table 1 Major Specifications

Transmit frequency	1,626.5~1,660.5MHz
Receive frequency	1,525.0~1,559.0MHz
Polarization	Right-hand circular
EIRP	13dBw
G/T	–14.6dB/K
Channel separation	6kHz
Frequency step size	500Hz
Modulation rate	3.375 kilobaud
Modulation	QPSK
Error correction	Convolution coding with K=7 and R 1/2 or R 3/4; Viterbi decoding
Voice codec	Improved multiband excitation, 6.4kbps
Data port	Asynchronous, 2,400 or 4,800bps
Standby time	8 hours

Table 2 Comparison of Terminal Equipment

Parameters	OmniQuest	ST150A
Weight	2.4kg	13.0kg
Dimensions	285 x 210 x 50mm (main unit)	356 x 356 x 108mm
Volume	3,000cc (main unit)	13,680cc
G/T	–14.6dB/K	–12dB/K
EIRP	13dBw	13dBw
Standby time	8 hours	8hours
Battery	3,100mAh nickel metal hydride	12,000mAh lead acid

and faced toward the satellite. The battery is an internally mounted nickel metal hydride type. The terminal unit contains a transceiver unit and an RF unit. The transceiver unit includes a converter board and a digital circuitry board. The transceiver unit is removable, and an optional mobile transceiver unit can be used for vehicle applications with an optional vehicle-mounted antenna. Table 1 lists the major specifications of the OmniQuest terminal.

When the terminal is used to transmit voice, the signal from the handset is digitized by a PCM codec and coded as a 6.4kbps audio signal by a DSP using an improved multiband excitation algorithm. The signal is then converted to the frame format required for the satellite link, a digital filter performs waveform correction, and circuitry on the converter board performs direct QPSK modulation. Finally, the QPSK signal is applied to a power amplifier and the amplified signal passed through the diplexer to the antenna for transmission to the satellite. A removable connector linking the diplexer to the antenna allows an external antenna to be used.

Received signals are amplified in a low-noise amplifier and converted to an IF signal in two steps by circuitry on the converter board, then digitized by an ADC. The digital IF signal is converted to a baseband signal, and filtering is performed. The DSP has functions for demodulating and deframing this digital signal and for decoding the voice signal. Multisymbol delayed detection and maximum likelihood sequence estimation techniques are used in demodulation for optimum performance under Rice fading.

When the terminal is in standby mode, it monitors a control signal from the satellite. This signal is convolutional coded with a constraint length of 7. The signal is demodulated by soft Viterbi decoding.

The frequency synthesizer achieves a combination of high-speed performance and extremely small 500Hz step size through using direct digital synthesis techniques with two phase-locked loops.

Table 2 compares the performance of the OmniQuest terminal with the corporation's ST150A terminal equipment. OmniQuest offers comparable performance with 22% of the volume and 18% of the weight in a triumph of miniaturization.

The OmniQuest terminal equipment represents a dramatic reduction in the size and weight of satellite terminals, achieving a fivefold improvement over the corporation's previous product. OmniQuest marks a significant step toward a future generation of handheld satellite terminals. ❑

MITSUBISHI ELECTRIC OVERSEAS NETWORK (Abridged)

Country	Address		Telephone
U.S.A.	Mitsubishi Electric America, Inc.	5665 Plaza Drive, P.O. Box 6007, Cypress, California 90630-0007	714-220-2500
	Mitsubishi Electric America, Inc. Sunnyvale Office	1050 East Arques Avenue, Sunnyvale, California 94086	408-731-3973
	Mitsubishi Electronics America, Inc.	5665 Plaza Drive, P.O. Box 6007, Cypress, California 90630-0007	714-220-2500
	Mitsubishi Consumer Electronics America, Inc.	9351, Jeronimo Road, Irvine, California 92618	949-465-6000
	Mitsubishi Semiconductor America, Inc.	Three Diamond Lane, Durham, North Carolina 27704	919-479-3333
	Mitsubishi Electric Power Products Inc.	512 Keystone Drive, Warrendale, Pennsylvania 15086	724-772-2555
	Mitsubishi Electric Automotive America, Inc.	4773 Bethany Road, Mason, Ohio 45040	513-398-2220
	Astronet Corporation	3805 Crestwood Parkway Suite 400 Duluth, Georgia 30096	770-638-2000
	Powerex, Inc.	Hills Street, Youngwood, Pennsylvania 15697	724-925-7272
	Mitsubishi Electric Information Technology Center America , Inc.	201 Broadway, Cambridge, Massachusetts 02139	617-621-7500
Canada	Mitsubishi Electric Sales Canada Inc.	4299 14th Avenue, Markham, Ontario L3R 0J2	905-475-7728
Mexico	Melco de Mexico S.A. de C.V.	Mariano Escobedo No. 69,Tlalnepantla, Edo. de Mexico Apartado Postal No.417, Tlalnepantla	5-565-4925
Brazil	Melco do Brazil, Com. e Rep. Ltda.	Av. Rio Branco, 123, S/1504-Centro, Rio de Janeiro, RJ CEP 20040-005	21-221-8343
	Melco-TEC Rep. Com. e Assessoria Tecnica Ltda.	Av. Rio Branco, 123, S/1507, Rio de Janeiro, RJ CEP 20040-005	21-221-8343
Argentina	Melco Argentina S.A.	Florida 890-20-Piso, Buenos Aires	1-311-4801
Colombia	Melco de Colombia Ltda.	Calle 35 No. 7-25, P.12 A. A. 29653 Santafe de Bogota, D.C.	1-287-9277
U.K.	Mitsubishi Electric U.K. Ltd. Livingston Factory	Houston Industrial Estate, Livingston, West Lothian, EH54 5DJ, Scotland	1506-437444
	Apricot Computers Ltd.	3500 Parkside, Birmingham Business Park, Birmingham, B37 7YS, England	121-717-7171
	Mitsubishi Electric Europe B.V. Corporate Office	Centre Point (18th Floor), 103 New Oxford Street, London, WC1A 1EB	171-379-7160
France	Mitsubishi Electric France S.A. Bretagne Factory	Le Piquet 35370, Etrelles	2-99-75-71-00
The Netherlands	Mitsubishi Electric Netherlands B.V.	3rd Floor, Parnassustoren, Locatellikade 1, 1076 AZ, Amsterdam	020-6790094
Belgium	Mitsubishi Electric Europe B.V. Brussels Office	Avenue Louise 125, Box 6, 1050 Brussels	2-534-3210
Germany	Mitsubishi Electric Europe B.V. German Branch	Gothaer Strasse 8, 40880 Ratingen	2102-4860
	Mitsubishi Semiconductor Europe GmbH	Konrad-Zuse-Strasse 1, D-52477 Alsdorf	2404-990
Spain	Mitsubishi Electric Europe B.V. Spanish Branch	Polígono Industrial "Can Magí", Calle Joan Buscallà 2-4, Apartado de Correos 420, 08190 Sant Cugat del Vallês, Barcelona	3-565-3131
Italy	Mitsubishi Electric Europe B.V. Italian Branch	Centro Direzionale Colleoni, Palazzo Persero-Ingresso 2, Via Paracelso 12, 20041 Agrate Brianza	39-60531
China	Mitsubishi Electric (China) Co., Ltd.	Room No. 1609 Scite Building (Noble Tower), Jianguo Menwai Street, Beijing	10-6512-3222
	Mitsubishi Electric (China) Co., Ltd. Shanghai Office	39th Floor, Shanghai Senmao International Building, 101, Yincheng Road (E), Pudong New Area, Shanghai	21-6841-5300
	Mitsubishi Electric (China) Co., Ltd. Guangzhou Office	Room No. 1221-4, Garden Tower, Garden Hotel, 368, Huanshi Dong Lu, Guangzhou	20-8385-7797
	Shanghai Mitsubishi Elevator Co., Ltd.	811 Jiang Chuan Road, Minhang, Shanghai	21-6430-3030
Hong Kong	Mitsubishi Electric (H.K.) Ltd.	41st Floor, Manulife Tower, 169 Electric Road, North Point	2510-0555
	Ryoden (Holdings) Ltd.	10th Floor, Manulife Tower, 169 Electric Road, North Point	2887-8870
	Ryoden Merchandising Co., Ltd.	32nd Floor, Manulife Tower, 169 Electric Road, North Point	2510-0777
Korea	KEFICO Corporation	410, Dangjung-Dong, Kunpo, Kyunggi-Do	343-51-1403
Taiwan	Mitsubishi Electric Taiwan Co., Ltd.	11th Floor, 88 Sec. 6, Chung Shan N. Road, Taipei	2-2835-3030
	Shihlin Electric & Engineering Corp.	75, Sec. 6, Chung Shan N. Road, Taipei	2-2834-2662
	China Ryoden Co., Ltd.	Chung-Ling Bldg., No. 363, Sec. 2, Fu-Hsing S. Road, Taipei	2-2733-3424
Singapore	Mitsubishi Electric Singapore Pte. Ltd.	152, Beach Road, #11-06/08, Gateway East, Singapore 189721	295-5055
	Mitsubishi Electric Sales Singapore Pte. Ltd.	307, Alexandra Road, #05-01/02, Mitsubishi Electric Building, Singapore 159943	473-2308
	Mitsubishi Electronics Manufacturing Singapore Pte. Ltd.	3000, Marsiling Road, Singapore 739108	269-9711
	Mitsubishi Electric Asia Co-ordination Centre	307, Alexandra Road, #02-02, Mitsubishi Electric Building, Singapore 159943	479-9100
Malaysia	Mitsubishi Electric (Malaysia) Sdn. Bhd.	Plo 32, Kawasan Perindustrian Senai, 81400 Senai, Johor Daruel Takzim	7-5996060
	Antah Melco Sales & Services Sdn. Bhd.	No.6 Jalan 13/6, P.O. Box 1036, 46860 Petaling Jaya, Selangor, Daruel Ehsan	3-755-2088
	Ryoden (Malaysia) Sdn. Bhd.	No. 14 Jalan 19/1, 46300 Petaling Jaya Selongar Daruel Ehsam	3-755-3277
Thailand	Kang Yong Watana Co., Ltd.	28 Krungthep Kreetha Road, Huamark, Bangkapi, Bangkok 10240	2-731-6841
	Kang Yong Electric Public Co., Ltd.	67 Moo 11, Bangna-Trad Road KM. 20, Bangplee, Samutprakarn 10540	2-337-2431
	Melco Manufacturing (Thailand) Co., Ltd.	86 Moo 4, Bangna-Trad Road KM. 23, Bangsaothong, Samutprakarn 10540	2-312-8350~3
	Mitsubishi Elevator Asia Co., Ltd.	700/86~92, Amata Nakorn Industrial Estate Park2, Moo 6, Bangna-Trad Road, Tambon Don Hua Roh, Muang District, Chonburi	38-213-170
	Mitsubishi Electric Asia Coordination Center (Thailand)	17th Floor, Bangna Tower, 2/3 Moo 14, Bangna-Trad Highway 6.5 Km, Bangkawe, Bang Plee, Samutprakarn 10540	2-312-0155~7
Philippines	International Elevator & Equipment, Inc.	K.m. 23 West Service Road, South Superhighway, Cupang, Muntinlupa, Metro Manila	2-842-3161~5
Australia	Mitsubishi Electric Australia Pty. Ltd.	348 Victoria Road, Rydalmere, N.S.W. 2116	2-9684-7777
New Zealand	Melco New Zealand Ltd.	1 Parliament St., Lower Hutt, Wellington	4-560-9100
Representatives			
Korea	Mitsubishi Electric Corp. Seoul Office	Daehan Kyoyuk Insurance Bldg., Room No. 2205, #1,1-ka, Chongno-ku, Seoul	2-732-1531~2
India	Mitsubishi Electric Corp. New Delhi Liaison Office	Dr. Gopal Das Bhawan (8th Floor), 28 Barakhamba Road, New Delhi 110001	11-335-2343
Viet Nam	Mitsubishi Electric Corp. Ho Chi Minh City Office	18th Floor, Sun Wah Tower, 115 Nguyen Hue Street, District 1, Ho Chin Minh City	8-821-9038

MITSUBISHI ELECTRIC CORPORATION
HEAD OFFICE: MITSUBISHI DENKI BLDG., MARUNOUCHI, TOKYO 100-8310, FAX 03-3218-3455